Conditioning of and Algorithms for Image Reconstruction from Irregular Frequency Domain Samples

Benjamin C. Lee

Dissertation Oral Defense
May 10, 2010

University of Michigan
Electrical Engineering: Systems
Chair: Prof. Andrew Yagle

Overview

- **Problem**
- Conditioning Approach
- Non-Iterative Approach
- Divide-and-Conquer Approach
- Conclusion

2-D Fourier Transform

- Images are 2-D functions of intensity.

Image

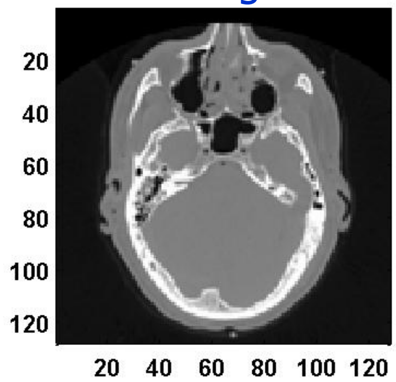

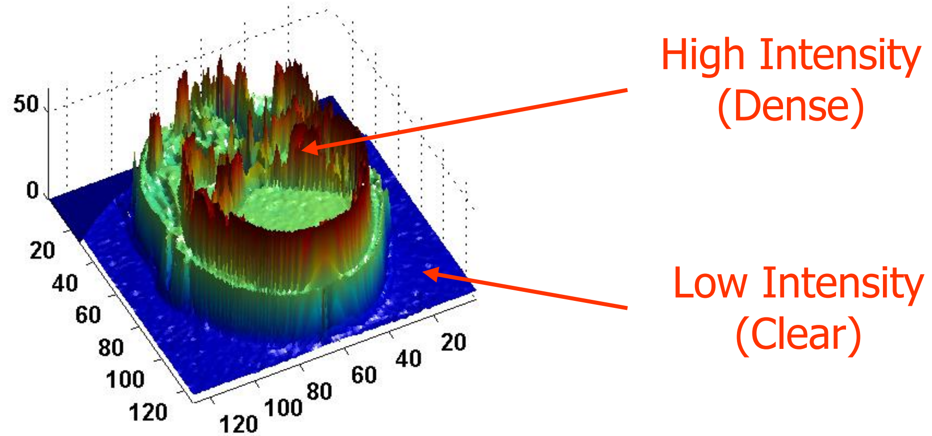

- Fourier Transform analyzes image in frequency domain.

2-D Fourier Transform

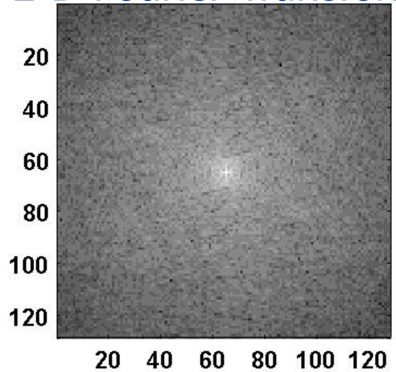

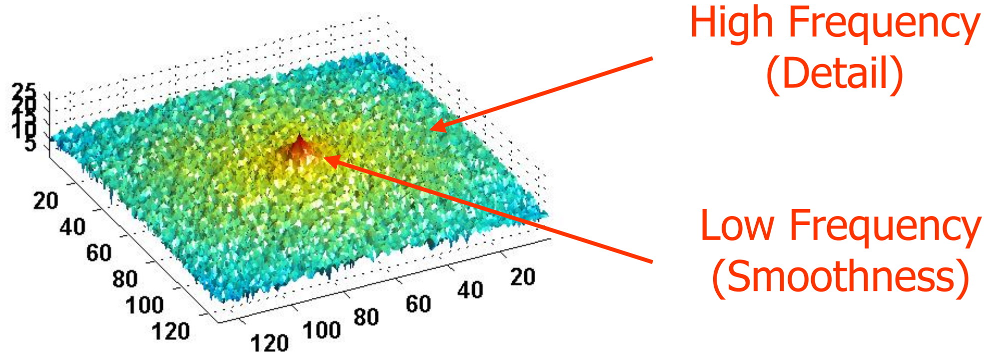

Head: www.lumen.luc.edu/lumen

Sampling Continuous-Space Images

- Given continuous image

$$x_C(s_1, s_2)$$

with 2-D Fourier Transform with wavenumbers k_1, k_2 *

$$X_C(k_1, k_2) = \int_{-\infty}^{\infty}\int_{-\infty}^{\infty} x_C(s_1, s_2) e^{-2\pi j(s_1 k_1 + s_2 k_2)} ds_1 ds_2$$

- Assume image is spatially bandlimited to wavenumber $\frac{1}{2\Delta}$
- Sampled image

$$x(i_1, i_2) = x_C(i_1\Delta, i_2\Delta)$$

with 2-D Discrete-Time Fourier Transform (DTFT) **

$$X(e^{j\omega_1}, e^{j\omega_2}) = \sum_{i_1=-\infty}^{\infty}\sum_{i_2=-\infty}^{\infty} x(i_1, i_2) e^{-j(i_1\omega_1 + i_2\omega_2)}$$

is now 2-D periodic in wavenumber.

* Also known as the Continuous-Space Fourier Transform (CSFT). ** Also known as the Discrete-Space Fourier Transform (DSFT).

Problem Statement

- Given some N values of the 2-D Discrete-Time Fourier Transform

$$\left\{ X(e^{j\omega_{1,k}}, e^{j\omega_{2,k}}), k = 1, \ldots, N \right\}$$

reconstruct its $M \times M$ image

$$x(i_1, i_2)$$

- Why not use inverse 2-D Discrete Fourier Transform (DFT)?
  - Only some 2-D DTFT values are known on 2-D rectangular grid.

Spotlight-Mode Synthetic Aperture Radar (SAR)

- Ground area is imaged from radar signals at many angles.

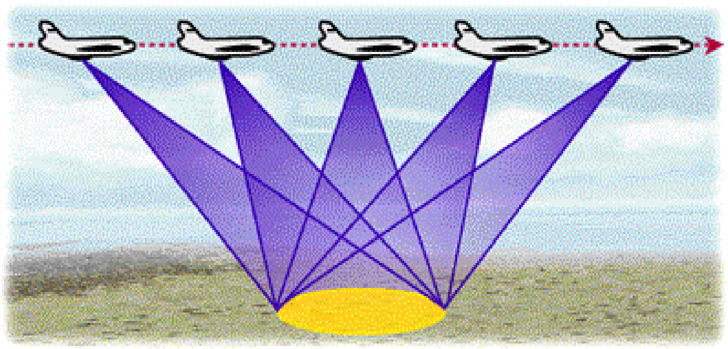

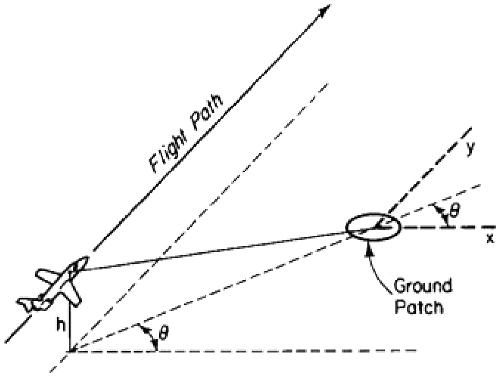

- 2-D DTFT is known on arcs.

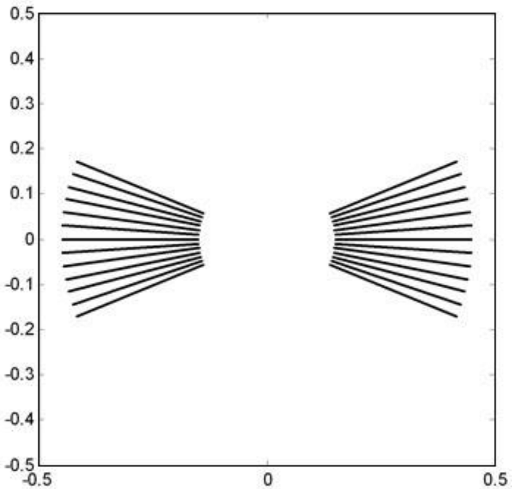

SAR Side View: www.ccrs.nrcan.gc.ca, SAR Image: www.sandia.gov/radar

Limited-Angle Tomography (LAT)

- Microscope transmits electrons through cells on slides.

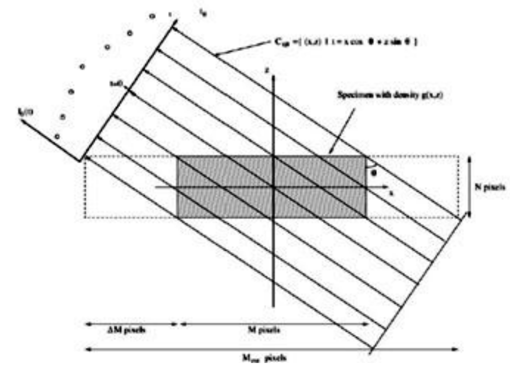

- 2-D DTFT is known on only some slices.

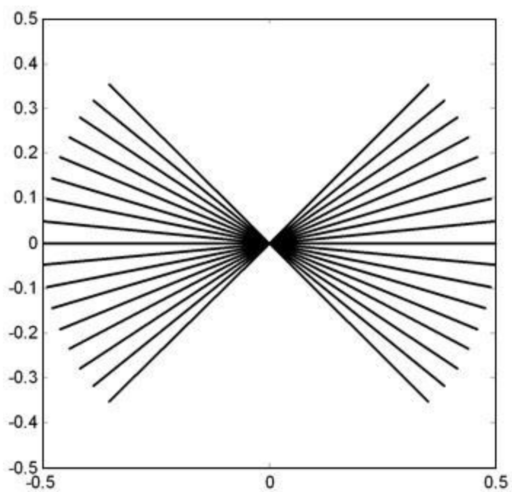

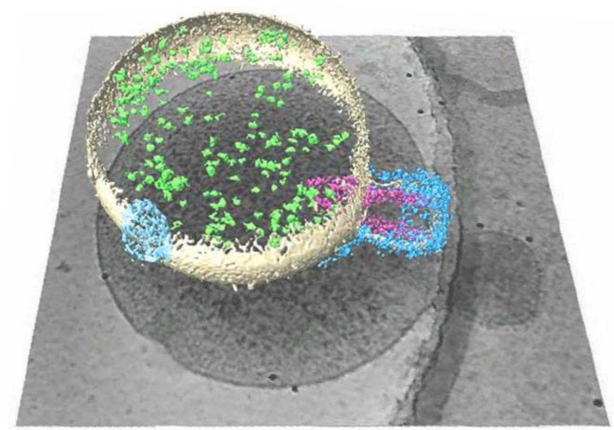

Microscope: www.electronmicroscopy.nl, Slide: Sandberg, J Struct Bio, 144 (2003) 61-72, Pneumonia Cell: www-db.embl.de/jss/EmblGroupsOrg/g_247.html

2-D Filter Design

- Filter is designed with a prescribed frequency response.

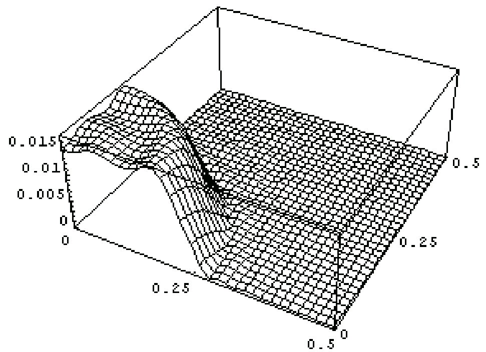

- 2-D DTFT is known on passband and stopband contours.

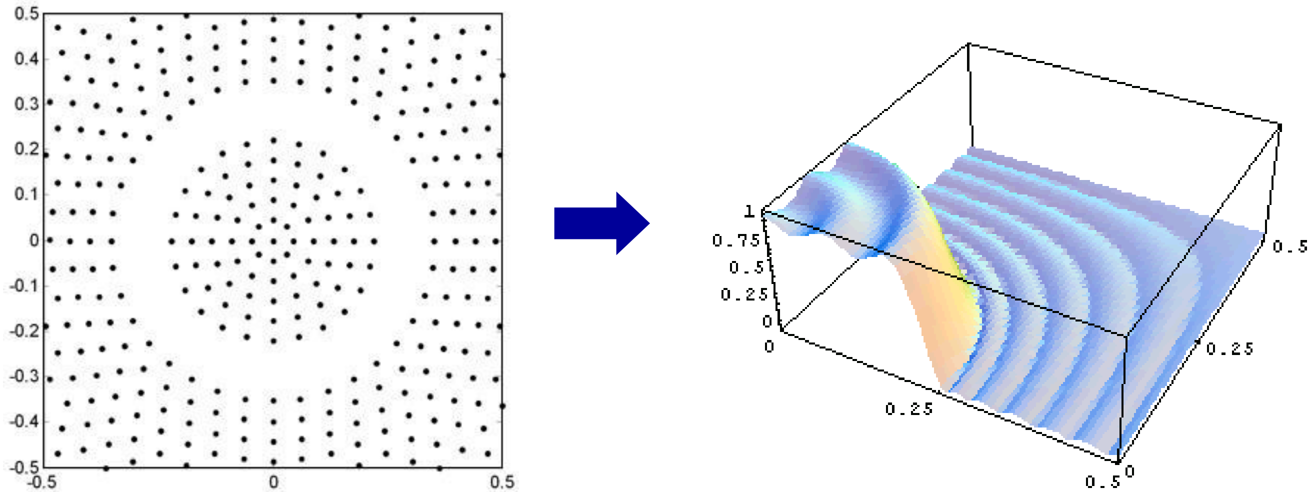

Spiral Scan Magnetic Resonance Imaging (MRI)

- Body is imaged from induced oscillating magnetic fields.

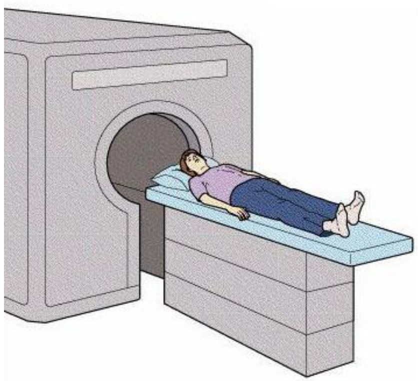

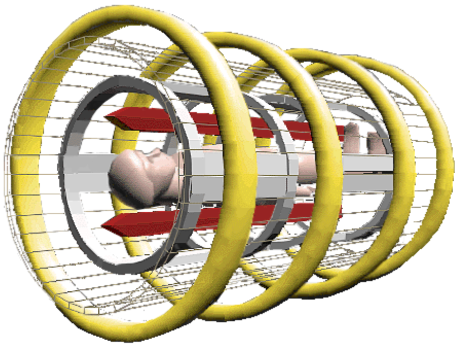

- 2-D DTFT is known on spiral trajectory.

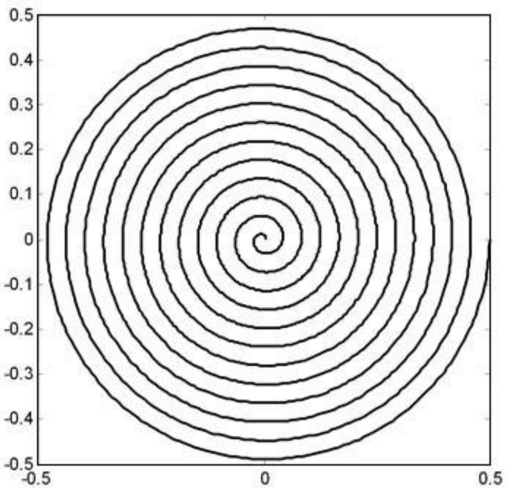

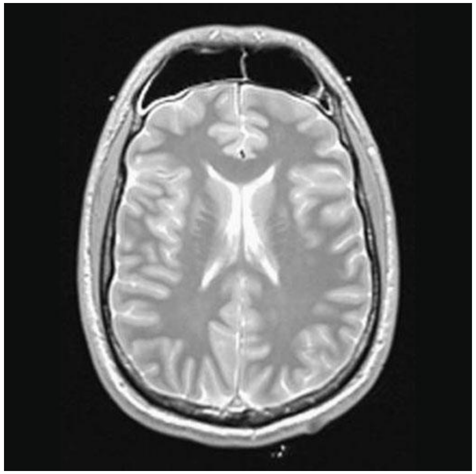

Machine: www.e-radiography.net, Coils: www.med.yale.edu/intmed/cardio/imaging, Image: www.lumen.luc.edu/lumen

Computed Tomography (CT)

- Body is imaged from rotating fan-beam x-ray projections.

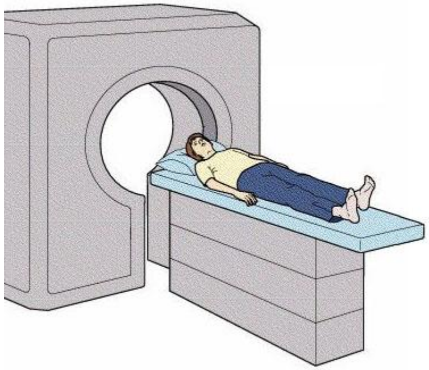

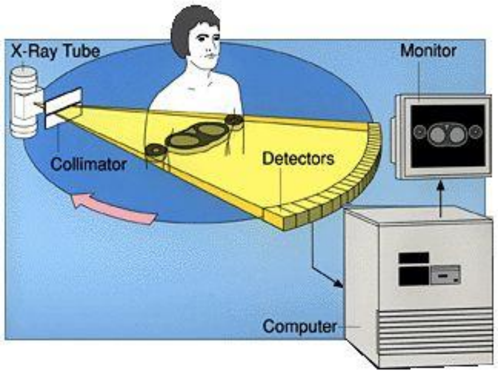

- After rebinning, 2-D DTFT is known on slices over 360°.

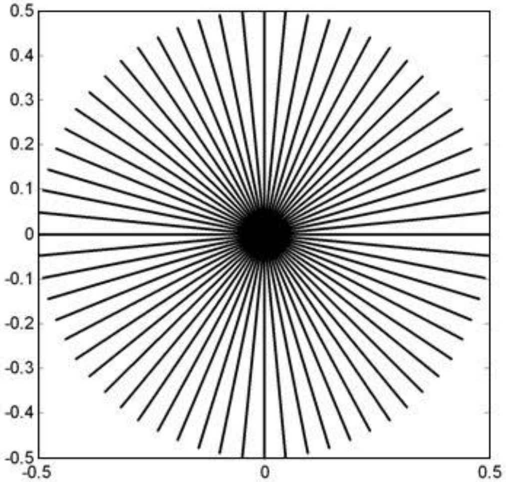

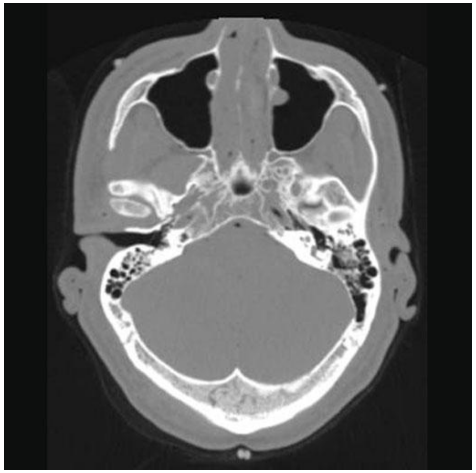

Machine: www.e-radiography.net, XRay: www.imaginis.com, Image: www.lumen.luc.edu/lumen

Filtered Back-Projection (FBP)

- Filtered back-projection only <u>approximates</u> (but still good).

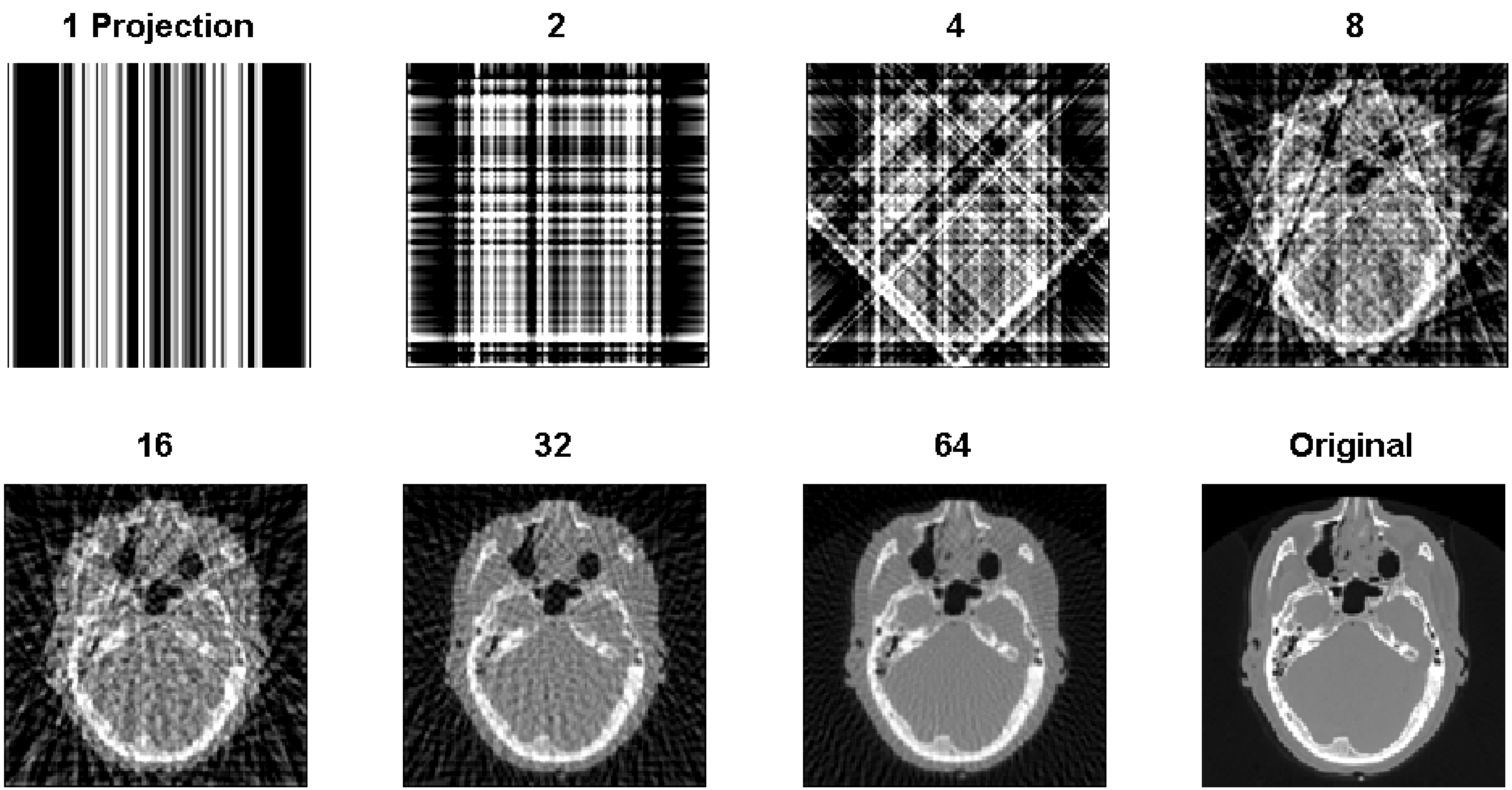

Direct Fourier Inversion (Gridding)

- Interpolate frequency values over whole grid from slices, then take inverse 2-D Fourier transform.

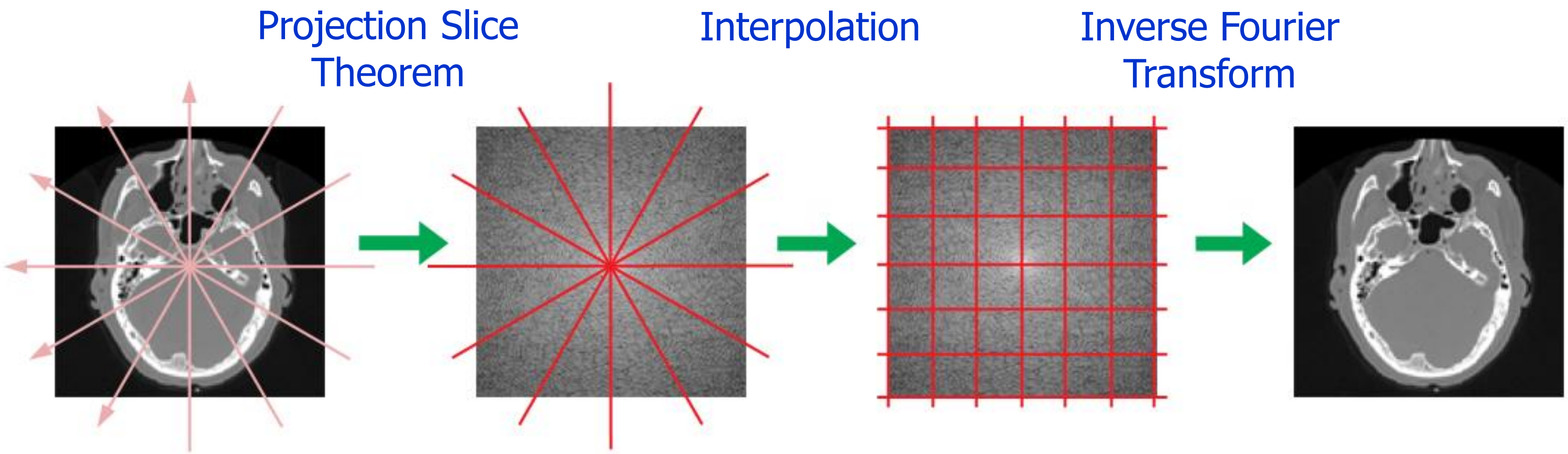

- But once again this is still an approximation. Is there an exact solution?
  - Yes

Head: www.lumen.luc.edu/lumen

System of Linear Equations

- Why not solve as large system of linear equations?

$$Ax = b$$

$$\begin{bmatrix} 1 & \cdots & e^{-j(M-1)(\omega_{1,1}+\omega_{2,1})} \\ \vdots & \ddots & \vdots \\ 1 & \cdots & e^{-j(M-1)(\omega_{1,N}+\omega_{2,N})} \end{bmatrix} \begin{bmatrix} x(0,0) \\ \vdots \\ x(M-1,M-1) \end{bmatrix} = \begin{bmatrix} X(e^{j\omega_{1,1}}, e^{j\omega_{2,1}}) \\ \vdots \\ X(e^{j\omega_{1,N}}, e^{j\omega_{2,N}}) \end{bmatrix}$$

System Matrix (Frequency Locations) | Solution (Image) | Data (Frequency Values)

- This is an exact solution, but uniqueness (how many sufficient frequencies), conditioning (stability), determined by frequency locations and algorithm choice, are unclear in 2-D.

Uniqueness

- How many 1-D DTFT values are sufficient to ensure that a 1-D signal is uniquely determined?
  - Just M (support size).

- How many 2-D DTFT values

$$\left\{X(e^{j\omega_{1,k}}, e^{j\omega_{2,k}}), k = 1, \ldots, N\right\}$$

are sufficient to ensure that the $M \times M$ image

$$x(i_1, i_2)$$

is uniquely determined?
  - In some cases, more than M^2.

Conditioning

- On what set of projection angles should data be collected?

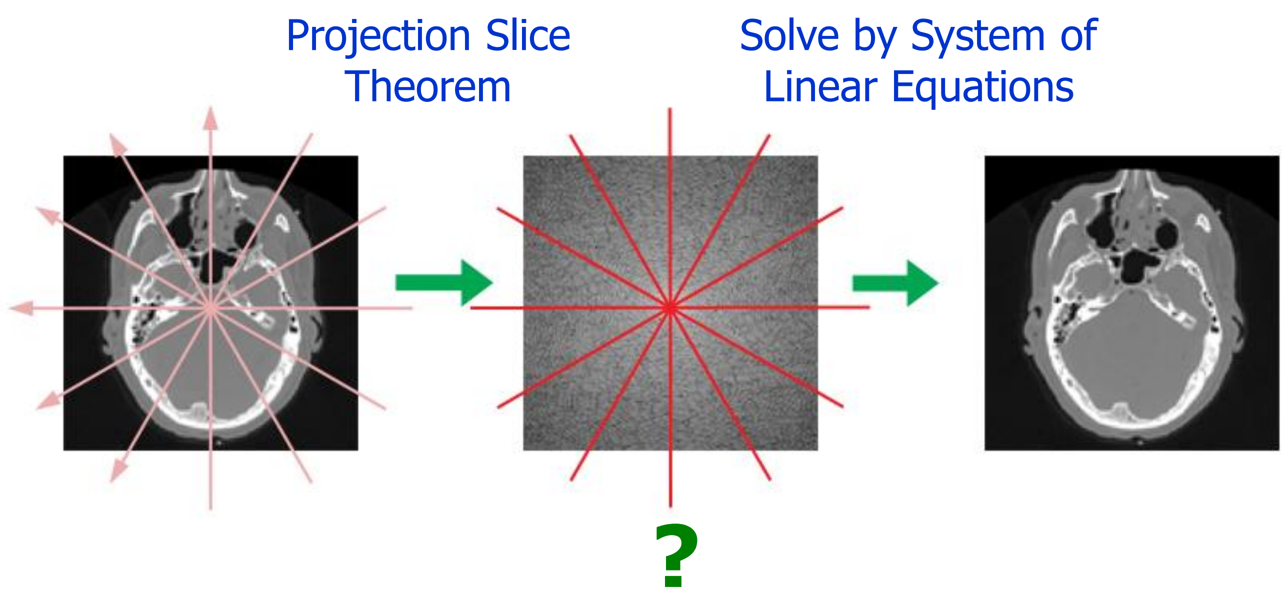

- One that leads to the least amount of noise in the solution.

Head: www.lumen.luc.edu/lumen

Conditioning

- Sensitivity of the solution to perturbations in the data.
  - Noise in the frequency data is amplified in reconstructed image.
  - Condition number of system matrix determines noise amplification.
  - Conditioning depends on frequency locations in system matrix.

$$A(x+\varepsilon)=b+\delta$$

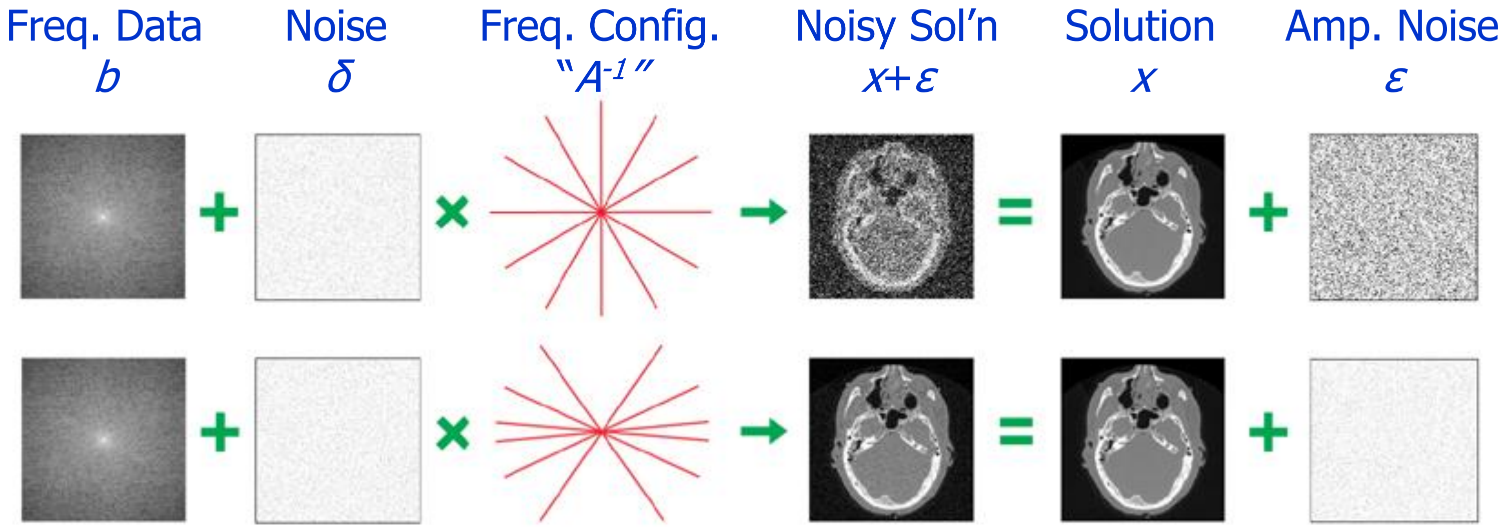

Head: www.lumen.luc.edu/lumen

Reconstruction Method

1. Cost Function: "What are we solving?"
   - Minimize: Cost function = Data-fit term + Regularization term *
   - How many data samples? (uniqueness)
     - Square or "just-determined" system
     - Over-determined system
   - How is noise handled? (conditioning)
     - Regularization
     - Well-conditioned frequency selection

$$A\hat{x} = b$$

$$(A^H A)\hat{x} = A^H b$$

$$(A^H A + \lambda^2 I)\hat{x} = A^H b$$

$$(\tilde{A}^H \tilde{A})\hat{x} = \tilde{A}^H \tilde{b}$$

2. Optimization Algorithm: "How do we solve it?"
   - Closed-form formula
   - Iterative method
   - Non-iterative method
   - Divide-and-conquer method

* Examples shown are linear least squares estimation solutions.

Goals

- To develop a simple procedure for evaluating the relative conditioning of various configurations of given 2-D DTFT samples without having to compute the condition number of the system matrix.
- To develop a fast algorithm to reconstruct an image by performing iterative computations offline once and then reapplying the method in one step to any measurement data with the same 2-D DFT configuration.
- To develop a partitioning procedure to break up a large reconstruction problem in to many smaller ones to reduce computation time or memory usage, or when a partial reconstruction is sufficient.

Previous Work

- Uniqueness
  - 2-D DTFT on lines [Zakhor '90, Zakhor '92]
  - Unwrapping to 1-D [Bresler '96, Yagle '00]
- Reconstruction
  - Projection onto Convex Sets [Youla '82]
  - Solve band-limited lexicographic 2-D system [Strohmer '97]
  - Non-uniform FFT interpolation [Fessler '03]
- Sparsifiable Image Model [Candes '06, Gilbert '06]
  - Requires random frequency locations
  - Requires linear programming or orthogonal matching pursuit
  - Outside scope of problem considered in this thesis

My Contributions

- Conditioning
  1. Computed closed-form expression for condition number and its upper bound of a just-determined problem using the Lagrange interpolation formula.
  2. Developed the variance measure as an accurate and fast estimate of conditioning not restricted to the just-determined case.
  3. Implemented simulated annealing with the variance sensitivity measure as the objective function in order to find well-conditioned frequency configurations.
  4. Developed 45° rotated image support Kronecker substitution reconstruction method with a unique 2-D to 1-D mapping for which the system matrix is smaller to solve.
  5. Showed non-rectangular regular 2-D DTFT configuration that is perfectly conditioned when unwrapped to 1-D.

My Contributions

- Algorithms

6. Introduced fast non-iterative DFT-based image reconstruction algorithm that deconvolves a precomputed filter from filtered data using just three 2-D DFTs.
7. Precomputed the filter using a finite-support constraint but which converges faster than POCS based on the dual of band-limited image interpolation.
8. Introduced a divide-and-conquer image reconstruction method using subband decomposition using Gabor filters.
9. Presented results of varying the amount of regularization or the over-determining factor for each subproblem separately with decreased error or computation time.
10. Applied presented reconstruction methods to actual CT sinogram data, provided by Adam M. Alessio of Univ. of Washington by the way of Jeffrey A. Fessler of Univ. of Michigan.

Overview

- Problem
- **Conditioning Approach**
- Non-Iterative Approach
- Divide-and-Conquer Approach
- Conclusion

Unwrapping from 2-D to 1-D

- Kronecker substitute

$$x = z^{(M-1)/2}, \quad y = z^{(M+1)/2}$$

in 2-D z-transform of 45° rotated support image

$$I(x,y) = a_0 x^0 y^3 + a_1 x^1 y^2 + a_2 x^2 y^1 + \ldots + a_{14} x^{-1} y^{-2} + a_{15} x^0 y^{-3}$$

$$\rightarrow I(z) z^{-7.5} = a_0 z^0 \quad + a_1 z^{-1} \quad + a_2 z^{-2} \quad + \ldots + a_{14} z^{-14} \quad + a_{15} z^{-15}$$

- 2-D DTFT samples constrained on 2-D periodic line

$$\omega_Y = \frac{M+1}{M-1} \omega_X$$

where they now map to 1-D

$$e^{j\omega} = e^{j(\omega_Y - \omega_X)} = \frac{y}{x} = z$$

- Solved 1-D signal is wrapped back to 2-D with index

$$i = \frac{M-1}{2} i_X + \frac{M+1}{2} i_Y$$

2-D DTFT Samples on Parallel Lines

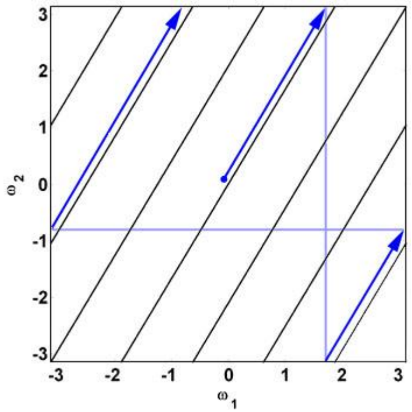

Rotated Support Image

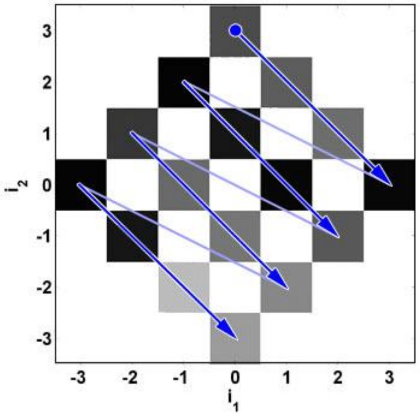

Variance Sensitivity Measure

- In 1-D, conditioning is easier to determine.
  - Condition number: $O(M^3)$, r=1.0

    $$\kappa_F^2(A) = \|A\|_F^2 \|A^{-1}\|_F^2 = M \sum_{m=1}^{M} \sum_{k=1}^{M} \left| \prod_{l=1, l\neq k}^{M} \frac{u_m - z_l}{z_k - z_l} \right|^2, \quad z_k = e^{j\omega_k}$$
  - Upper bound: $O(M^2)$, r=0.9

    $$\kappa_F^2(A) \le M^2 \sum_{k=1}^{M} \prod_{l=1, l\neq k}^{M} \frac{2}{1-\cos(\omega_k - \omega_l)}$$
  - Variance measure *: $O(M)$, r=0.8 **

    $$\sigma_\kappa^2(A) = M \sum_{k=1}^{M} \left(|\omega_{k+1} - \omega_k| - \mu \right)^2$$

$$\mu = \frac{1}{M} \sum_{k=1}^{M} |\omega_{k+1} - \omega_k|, \quad \omega_1 < \omega_2 < \ldots < \omega_{M+1} = \omega_1 + 2\pi$$

* Normalized variance of distances between adjacent frequency locations measures departure from a uniform distribution.
** Sample correlation coefficient (r) between the variance measure and the condition number in the over-determined case.

Frequency Selection

- Variance measure relatively determines if a frequency configuration leads to a well-conditioned system.

2-D

1-D

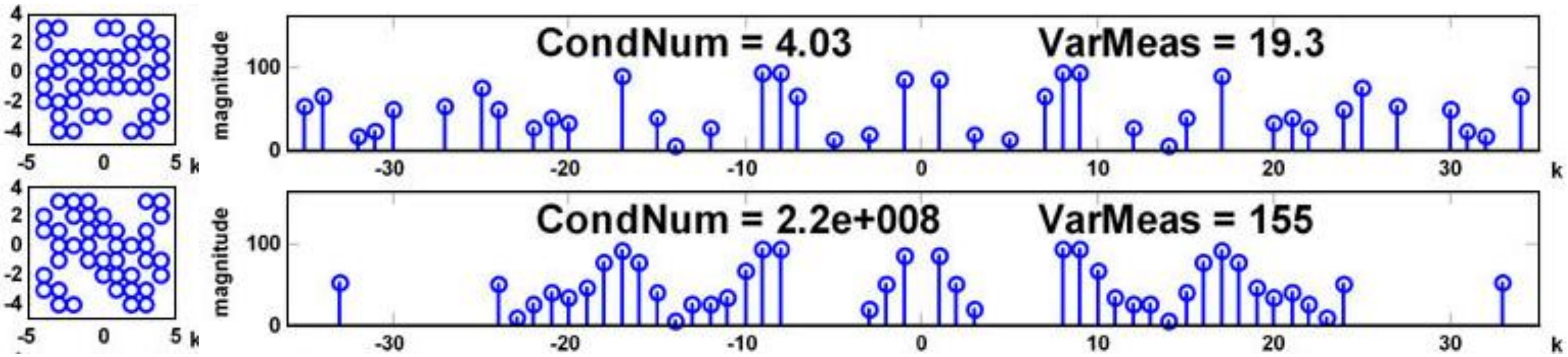

- How do we find such a configuration?
  - Simulated annealing uses the variance measure as its cost function to find a global minimum, in the case of CT, a near-optimal angle configuration.

2-D DTFT Intersections

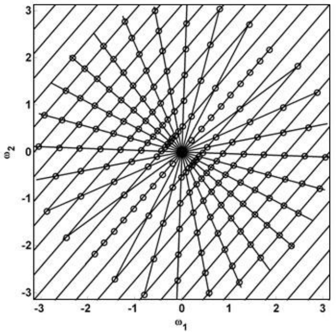

Frequency Configuration Example

- M=31 band-limited diagonals intersecting with CT slices.
  - The baseline uniform-angle configuration has 44 slices intersecting at 973 data samples and variance measure of 27.7.
  - The near-optimal variable-angle configuration has 68 slices intersecting at 969 data samples and variance measure of 11.2.

Uniform-Angle Projections → High-Variance DTFT Locations

Variable-Angle Projections → Low-Variance DTFT Locations

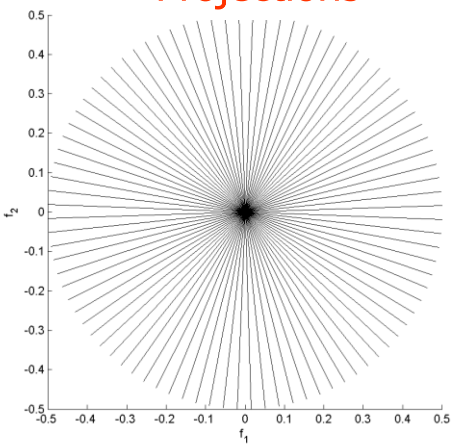

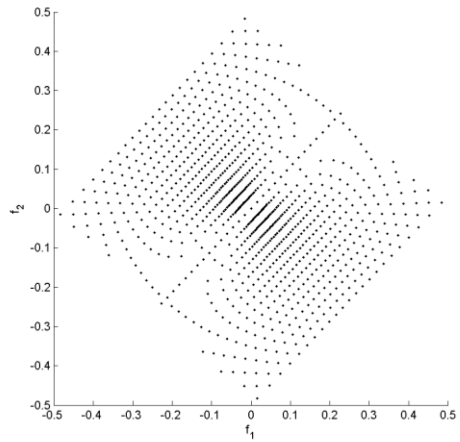

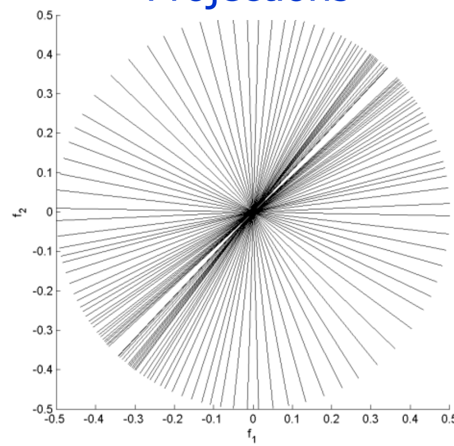

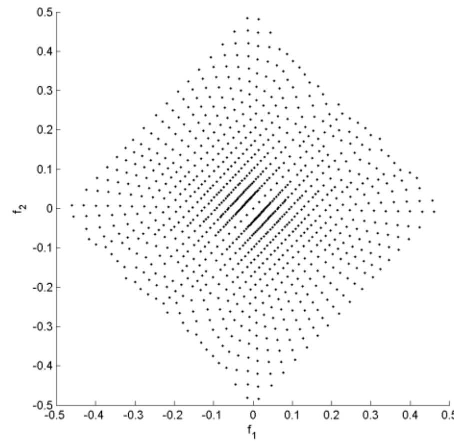

Simulation Data Frequency Configuration

- Simulation data slices intersect 255 diagonal lines at 64,264 samples.
- Image has size $M \times M$ =253×253 and 1-D solution has support 32,131.
- Given 1-D DTFTs, minimize over-determined non-regularized costs:

$$\Phi(x) = \left\| Ax - b \right\|^2 \qquad \tilde{\Phi}(x) = \left\| \tilde{A}x - \tilde{b} \right\|^2$$

Uniform-Angle Configuration
(VarMeas = 61.7)

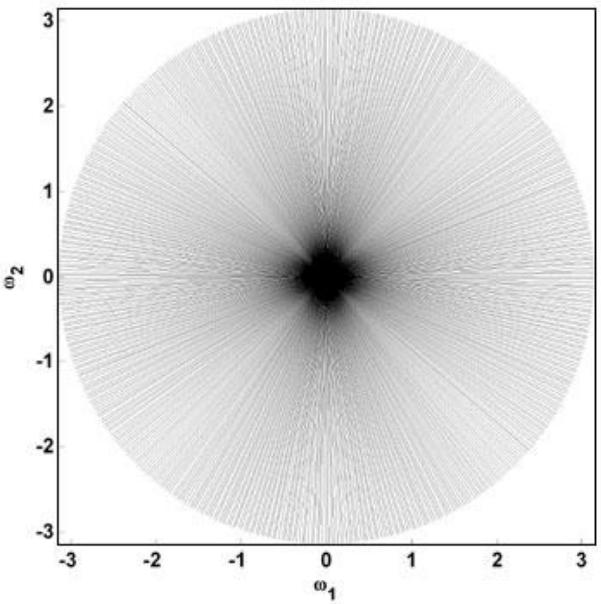

Variable-Angle Configuration
(VarMeas = 21.8)

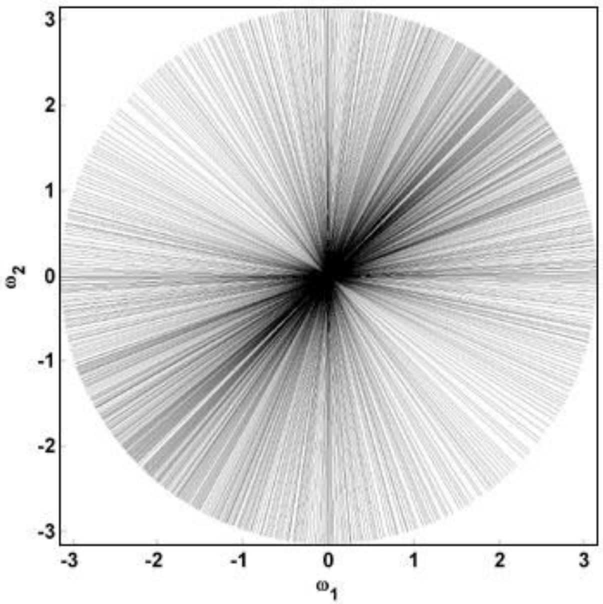

Simulation Data Reconstructed Images

- Each system is solved iteratively using preconditioned conjugate gradient (PCG) method with convergence tolerance of 1×10^{-6}.

$$(A^H A)\hat{x} = A^H b \qquad (\tilde{A}^H \tilde{A})\hat{x} = \tilde{A}^H \tilde{b}$$

Uniform-Angle Reconstruction
(RMSE = 3.91)

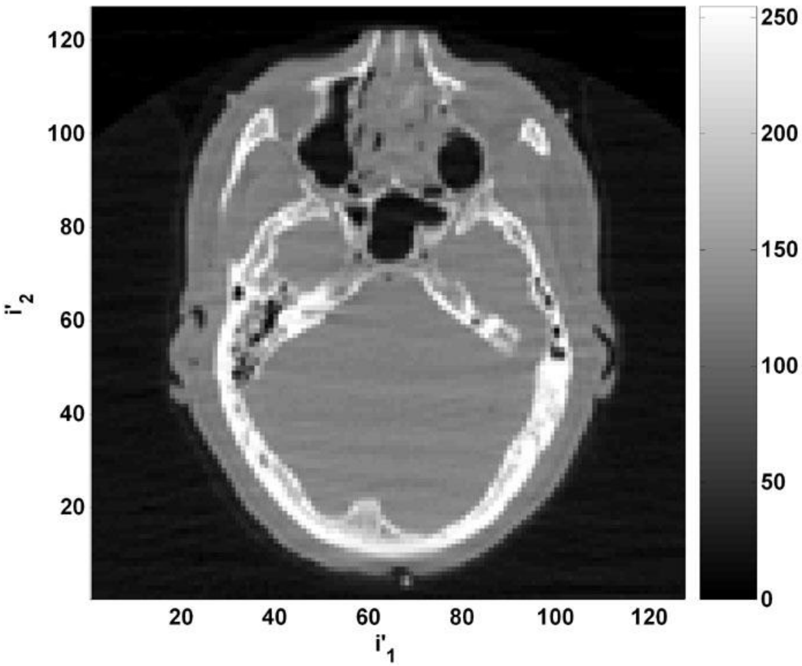

Variable-Angle Reconstruction
(RMSE = 1.22)

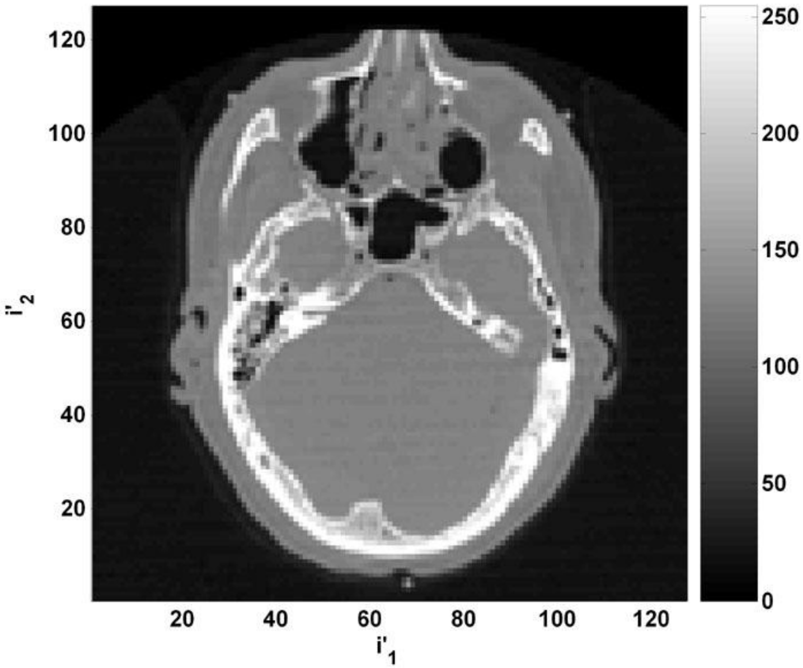

Simulation Data Performance

- Relative residual error versus PCG iteration
  - Uniform-angle configuration requires 203 iterations.
  - Variable-angle configuration requires 134 iterations.

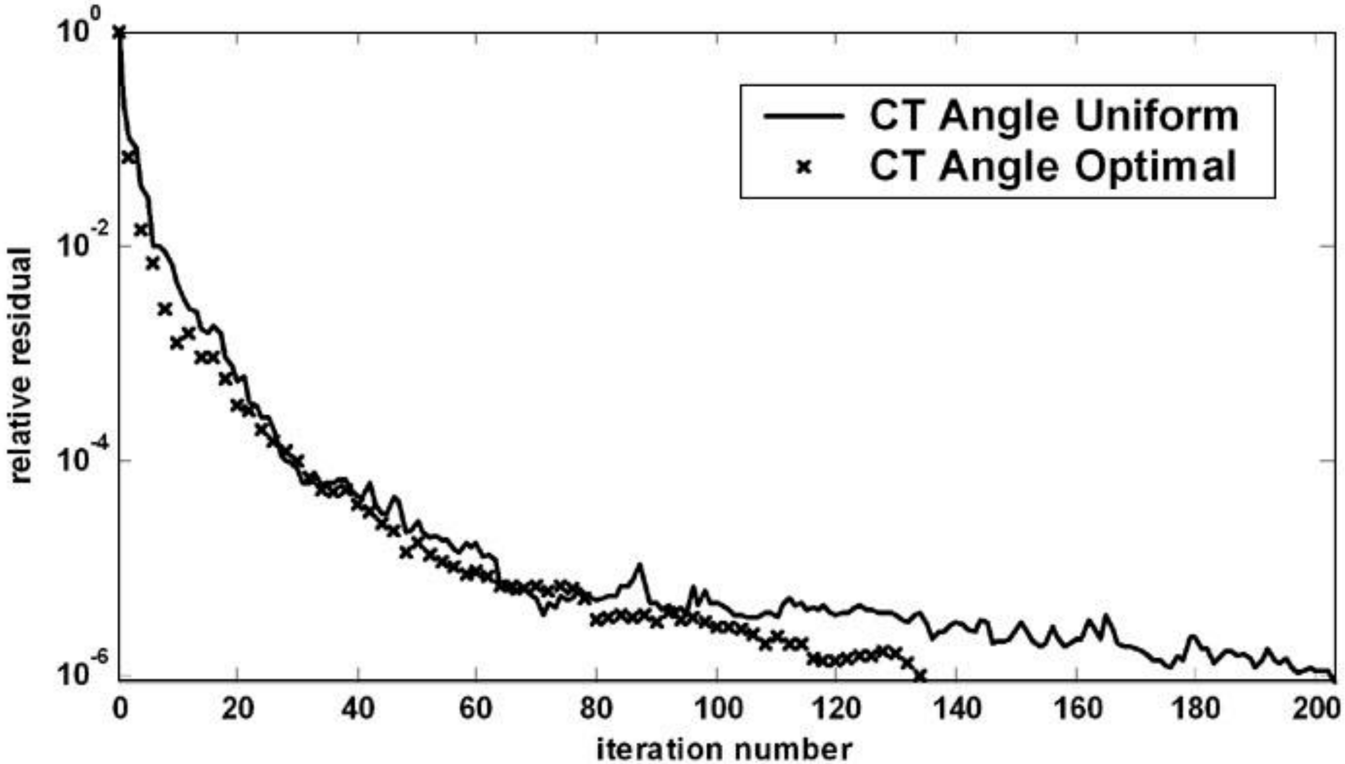

Actual CT Data

- Actual CT sinogram data* is rebinned
  - From fan beam with 820 projections over 360° and 888 detectors
  - To parallel beam with 410 projections over 180° and 889 detectors.
  - A reference FBP reconstructed image is shown to the right.

Fan Beam Sinogram

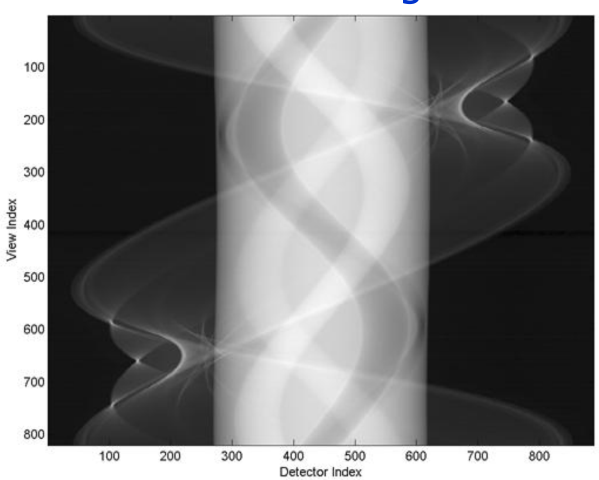

Parallel Beam Sinogram

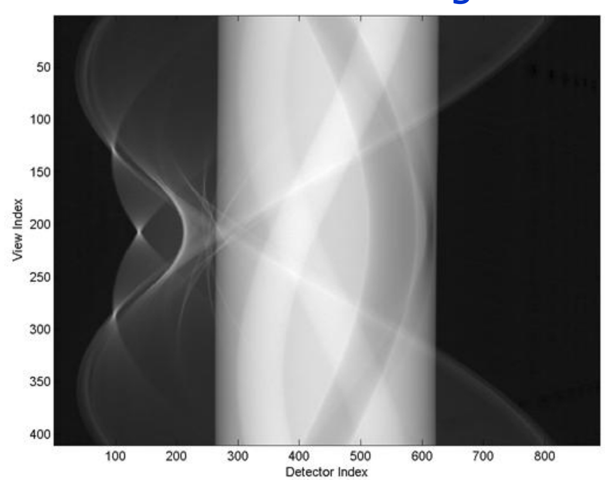

FBP Image

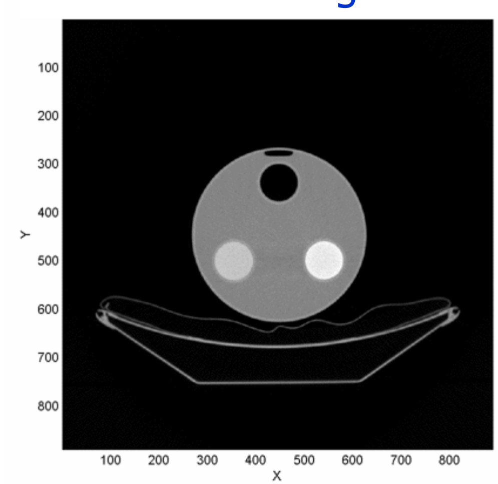

* Courtesy of Adam M. Alessio of the University of Washington by the way of Jeffrey A. Fessler of the University of Michigan.

Actual CT Reconstructed Images

- Actual CT data slices intersect M=255 band-limited diagonals.
  - The baseline uniform-angle configuration has 355 slices intersecting at 65,137 data samples and variance measure of 57.8.
  - The near-optimal variable-angle configuration has 527 slices intersecting at 65,095 data samples and variance measure of 27.4.
- Image has size 255×255 and 1-D solution has support 65,025.

FBP Image*

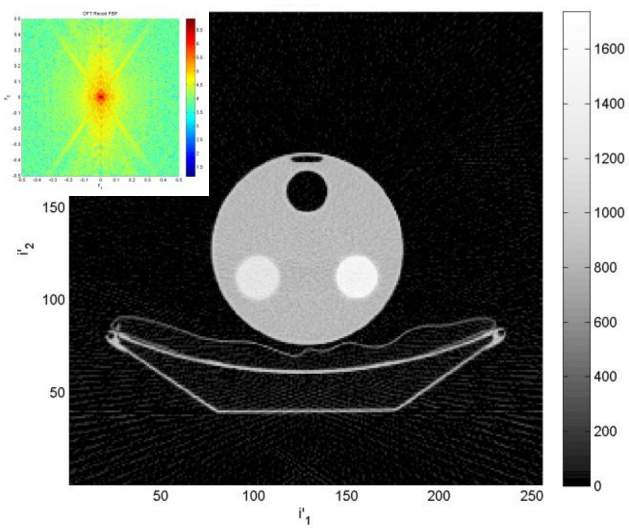

Uniform-Angle PCG Image

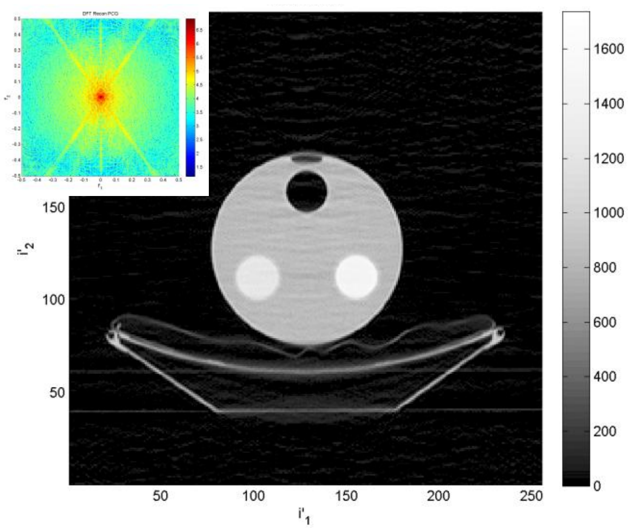

Variable-Angle PCG Image

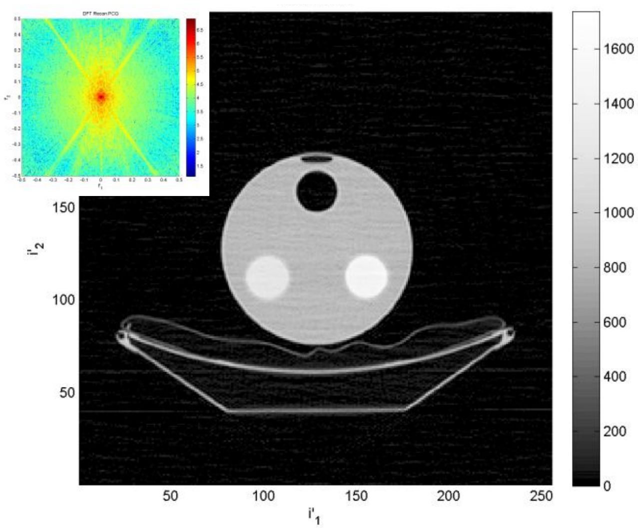

* Reference FBP image reconstructed from 128 uniform slices with 509 bins each and a non-apodized ramp filter.

Overview

- Problem
- Conditioning Approach
- **Non-Iterative Approach**
- Divide-and-Conquer Approach
- Conclusion

Why Non-Iterative?

- Iterative reconstructions algorithms are computationally expensive.
  - Projection Onto Convex Sets (POCS) requires many iterations to converge.
  - Preconditioned Conjugate Gradient (CG) method converges quicker but each iteration is slow.
- Solving normal equation has worse conditioning.
  - The condition number of $A^H A$ is square of condition number of A, which amplifies noise and can require drastic regularization.
  - CG iterations increases roughly with condition number even with help of preconditioning.

Modified Problem Statement

- Given some values of the $N \times N$ 2-D Discrete Fourier Transform (DFT)

$$X(k_1,k_2)=\sum_{i_1=0}^{N-1}\sum_{i_2=0}^{N-1}x(i_1,i_2)e^{-j\frac{2\pi}{N^2}(i_1k_1+i_2k_2)}$$

reconstruct its $M \times M$ image

$$x(i_1,i_2)$$

where $N >> M$.

- Why not use the inverse 2-D DFT this time?
  - Not all 2-D DFT values are known on the 2-D rectangular grid.

Algorithm

- DFT-based Deconvolution using a Data Masking Filter
  1. Precompute a filter with zero magnitude response at unknown 2-D DFT sample locations.

$$H(k_1,k_2)=0, \quad (k_1,k_2)\notin \Omega_{KNOWN}$$
$$h(i_1,i_2)=0, \quad (i_1,i_2) \notin \Pi_{SUPPORT}$$

  2. Filter known 2-D DFT samples in the frequency domain and set to zero elsewhere.

$$Y(k_1,k_2)=\begin{cases} H(k_1,k_2)\cdot X(k_1,k_2), & (k_1,k_2)\in\Omega_{KNOWN} \\ 0, & (k_1,k_2)\notin\Omega_{KNOWN} \end{cases}$$
$$y(i_1,i_2)=F^{-1}\{\, Y(k_1,k_2)\,\}$$

  3. Deconvolve original image from filtered image y using three 2-D DFT operations where g is the inverse filter. †

$$\hat{x}(i_1,i_2)=g(i_1,i_2)**y(i_1,i_2)$$

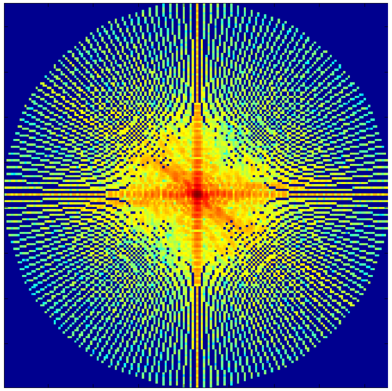

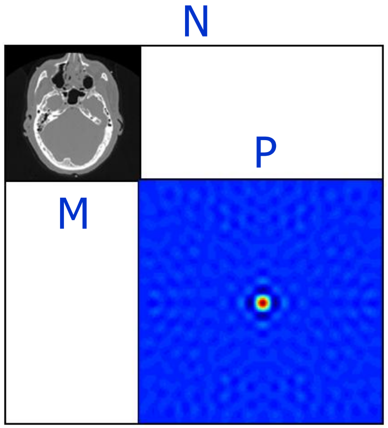

† Operator "**" denotes 2-D convolution.

Deconvolution

- Noisy system model in 2-D DFT domain is

$$H(k_1,k_2)\cdot X(k_1,k_2)=Y(k_1,k_2)+\eta(k_1,k_2)$$

- If no noise and $H(k_1,k_2)\neq 0$ then

$$X(k_1,k_2)=G(k_1,k_2)\cdot Y(k_1,k_2)=\frac{Y(k_1,k_2)}{H(k_1,k_2)}$$

- Tikhonov regularization numerically stabilizes solution

$$\hat{X}=\arg\min_X \left\|Y-H\cdot X\right\|^2+\lambda^2\left\|X\right\|^2$$

- Regularized inverse filter is then the Wiener filter

$$G(k_1,k_2)=\frac{1}{H(k_1,k_2)} \quad\rightarrow\quad \tilde{G}(k_1,k_2)=\frac{H(k_1,k_2)^*}{\left|H(k_1,k_2)\right|^2+\lambda^2}$$

- Deconvolution using 2-D DFTs of size L different from N

$$\hat{x}(i_1,i_2)=F_L^{-1}\left\{G_L(k_1,k_2)\cdot F_L\left\{F_N^{-1}\left\{Y_N(k_1,k_2)\right\}\right\}\right\}$$

* Additive white Gaussian noise.

Filter Design

- Filter Specification
  - $h(i_1,i_2) = 0$ for $N-M+1 \le i_1,\ i_2 \le N-1$
  - $H(k_1,k_2) = 0$ for (k_1,k_2) not in the set of Ω_{KNOWN}
- Filter Size
  - $h(i_1,i_2)$ unknown of size $P \times P = (N-M+1) \times (N-M+1)$
  - $h(i_1,i_2)$ known as 0 at $N^2 - P^2$ points
  - $H(k_1,k_2)$ arbitrarily known at $N^2 - P^2$ points
  - $H(k_1,k_2)$ known as 0 at P^2 points
  - Filter is unique since P^2 unknowns = P^2 equations
- Filtered Image
  - $y(i_1,i_2) = h(i_1,i_2) ** x(i_1,i_2)$ must be $N \times N$
  - Problem is over-determined by $(N^2 - P^2)/M^2 \approx 2N/M$

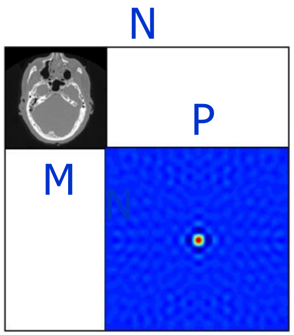

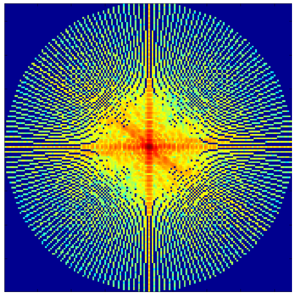

Filter Construction

- Projection Onto Convex Sets (POCS)
  - Alternatingly projects onto the spatial domain imposing finite support and on the DFT domain imposing the known DFT values.
  - Not much storage needed.
  - Slow convergence.
- Finite-Support Regularized Conjugate Gradient (FSR)
  - Finite-support constraint is implemented as regularization in the cost function minimally biases the solution.
  - Minimizing cost function using the conjugate gradient algorithm has faster convergence.
  - Adapted as the Fourier dual of the band-limited interpolation approach [Strohmer '97].
  - Although iteratively computed it is done offline and just once.

Filter Construction using Finite-Support Regularization

- Objective Function
  - The objective function includes a data-fit term of only elements in set Ω^C of missing 2-D DFT values and a regularization term including only elements in set Π^C of non-support spatial values

$$\Phi(h) = \left\| J_{\Omega^C} F h - H_{\Omega^C} \right\|^2 + \lambda^2 \left\| J_{\Pi^C} h - h_{\Pi^C} \right\|^2$$

    - where J is an irregular downsampling matrix, F is the 2-D DFT matrix, H_{Ω^c} are unknown DFTs, and h_{Ω^c} are non-support spatial values of 0.
  - Minimizing the objective function with respect to filter solution *h* leads to the regularized normal equation of the form

$$(F^H I_{\Omega^C} F + \lambda^2 I_{\Pi^C})\hat{h} = F^H J_{\Omega^C}^H H_{\Omega^C}$$

    - where J^H is an upsampling matrix and $I_{\Omega^c} = J_{\Omega^c}^H J_{\Omega^c}$ is an indicator matrix.

Filter Construction using Finite-Support Regularization

- Uniqueness
  - Typically, $M \times M$ samples of an $N \times N$ 2-D DFT are not sufficient to uniquely determine a $M \times M$ image. However it can be shown our added constraints where non-support spatial values are known combined with the sampled 2-D DFT values result in uniqueness.
- Preconditioning
  - Preconditioning the system can improve the convergence rate

$$P^{-1}(F^H I_{\Omega^C} F + \lambda^2 I_{\Pi^C})\hat{h} = P^{-1} F^H J_{\Omega^C}^H H_{\Omega^C}$$

  - One simple but effective preconditioner is to replace the masking diagonal matrix with a scaled identity matrix as such

$$P = F^H(\alpha I)F + \lambda^2 I_{\Pi^C} = \alpha I + \lambda^2 I_{\Pi^C}$$

    - where α = $\mathrm{tr}(I_{\Omega^c})$ / $\mathrm{tr}(I_{\Pi^c})$ = K/N^2 and K is the cardinality of Ω^C

Filter Construction using Finite-Support Regularization

- Optimization Algorithm
  - As the regularization parameter $\lambda \rightarrow \infty$, the non-support region goes to 0 and we solve the transformed preconditioned normal equation

$$\left(\tfrac{1}{\alpha} I_{\Pi} F^{H} I_{\Omega^{C}} F I_{\Pi} + I_{\Pi^{C}}\right) \hat{g} = \tfrac{1}{\sqrt{\alpha}} I_{\Pi} F^{H} J_{\Omega^{C}}^{H} H_{\Omega^{C}}$$

$$\hat{h} = \tfrac{1}{\sqrt{\alpha}} I_{\Pi} \hat{g}$$

    - where the P has been Cholesky decomposed.
  - Conjugate Gradient (CG) is used to the solve the above, where each iteration only requires only two 2-D DFT operations per CG iteration in O($N^2 log(N)$).
  - This final form gives the same answer as POCS, yet converges at the faster rate of the preconditioned CG method.

Simulation Data Configuration

- Simulation data on nearest neighbor analytical spiral with 44 revolutions and up to 512 angular samples per revolution on the DFT of size NxN=768x768, with conjugate symmetry.
- Image size MxM=128x128 is over-determined by 2.5.
- Filter size PxP=641x641 is over-determined by 1.3, no regularization, and no noise.*

Mask of 2-D DFT Samples

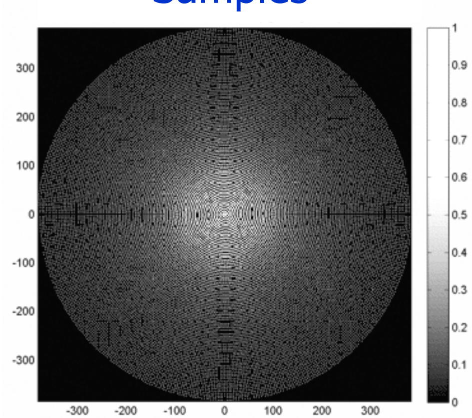

Log DFT of POCS Filter (Residual=3.3x10^{-3})

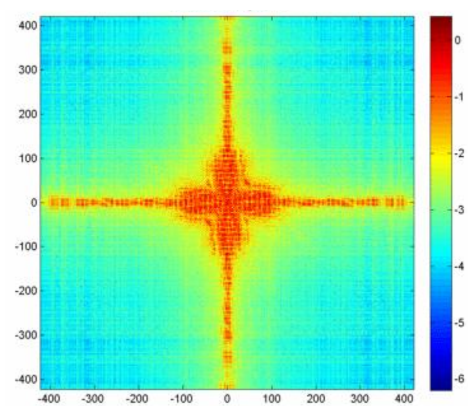

Log DFT of FSR Filter (Residual=2.8x10^{-3})

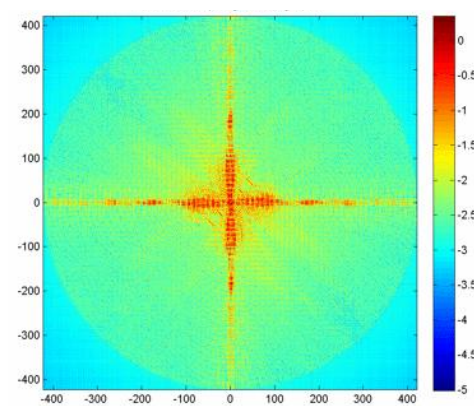

* Both POCS and FSR filters were generated with 250 iterations.

Simulation Data Reconstructed Images

- Deconvolution image size LxL=844x844.
- Approximate operations of POCS * is 5.2×10^7 in 5 iterations, Deconvolution (POCS Filter) is 2.1×10^7, and Deconvolution (FSR Filter) is 2.1×10^7.

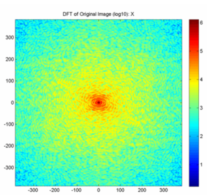

True DFT and Image RMSE=0.0

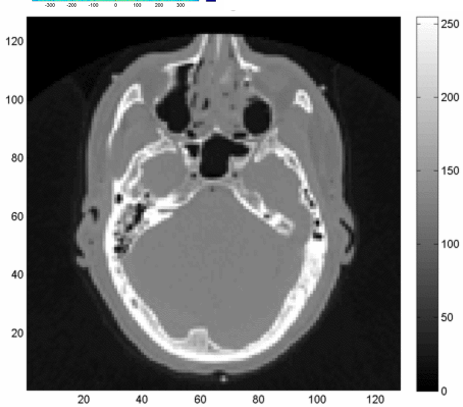

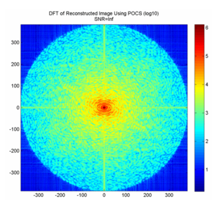

POCS Recon. DFT and Image RMSE=12.9

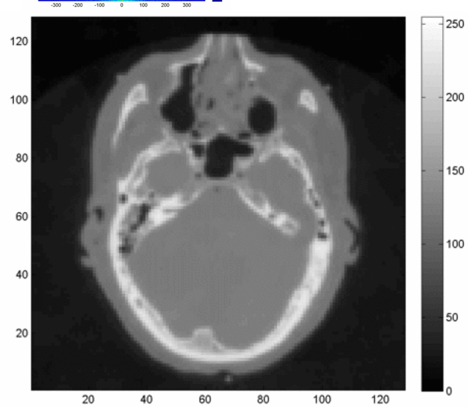

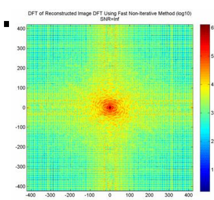

Deconv. DFT and Image (POCS Filter) RMSE=27.4

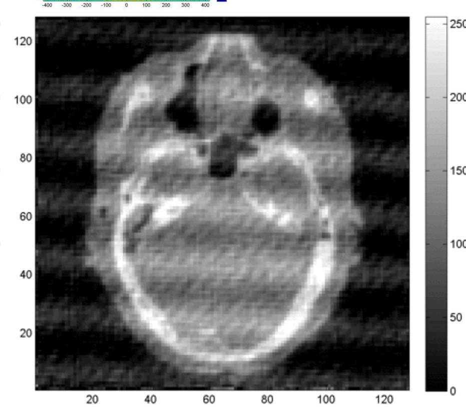

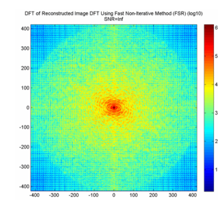

Deconv. DFT and Image (FSR Filter) RMSE=13.2

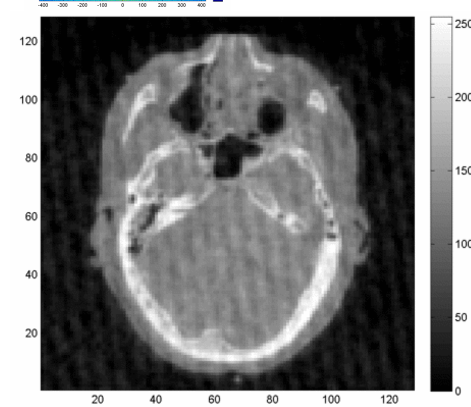

* POCS was stopped when RMSE was approximately that of the FSR-filtered deconvolution method and did <u>not</u> run to convergence.

Simulation Data Reconstruction Performance

- RMSE versus approximate operations of reconstruction methods including deconvolution using over-determined POCS-filter and FSR-filter.

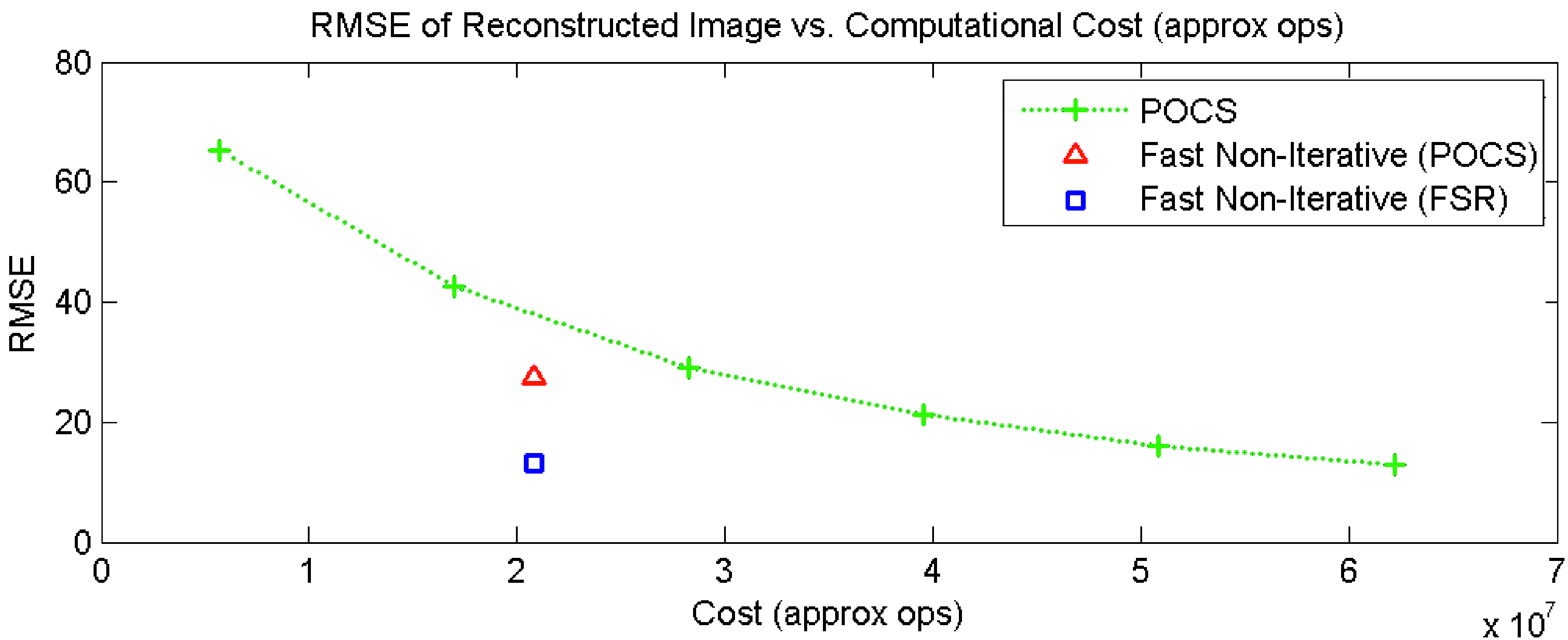

Actual CT Medium Configuration

- Actual CT data with 369 slices fill the DFT size NxN=1024x1024, with zeros beyond circular band-limit.
- Image size MxM=256x256 is over-determined by 6.9.
- Filter size PxP=769x769 is over-determined by 1.0, regularization $\lambda=1\times10^{-2}$, and no noise. *

Mask of 2-D DFT Samples

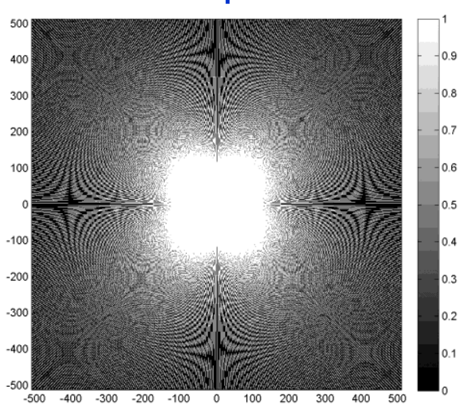

Log DFT of Filter H

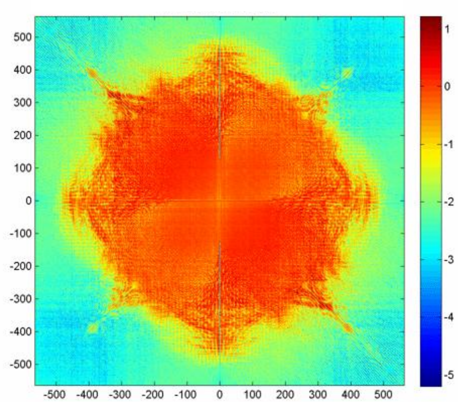

Log DFT of Inverse Filter G

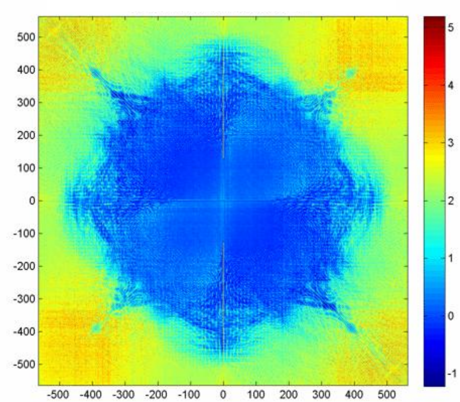

Log DFT of Regularized Inverse Filter

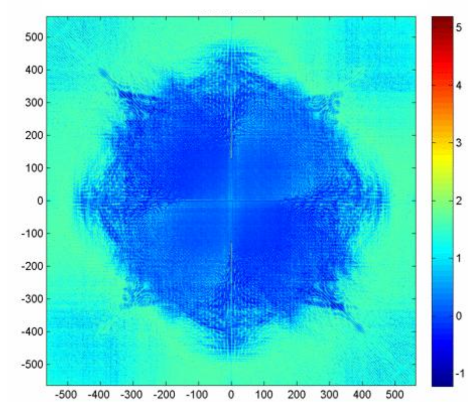

* Filter took 6 minutes to precompute offline.

Actual CT Medium Reconstructed Images

- Deconvolution image size LxL=1128x1128.
- Runtimes of POCS * is 1.4s in 3 iterations, Deconvolution is 1.2s, and Regularized Deconvolution is 1.2s.

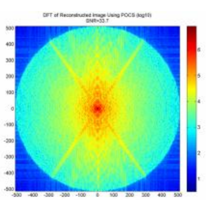

POCS DFT and Zoomed Image

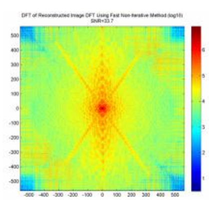

Deconv. DFT and Zoomed Image

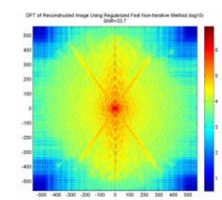

Reg. Deconv. DFT and Zoomed Image

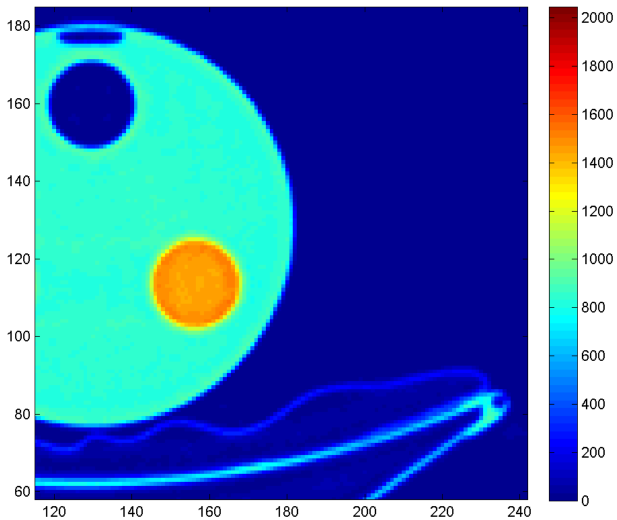

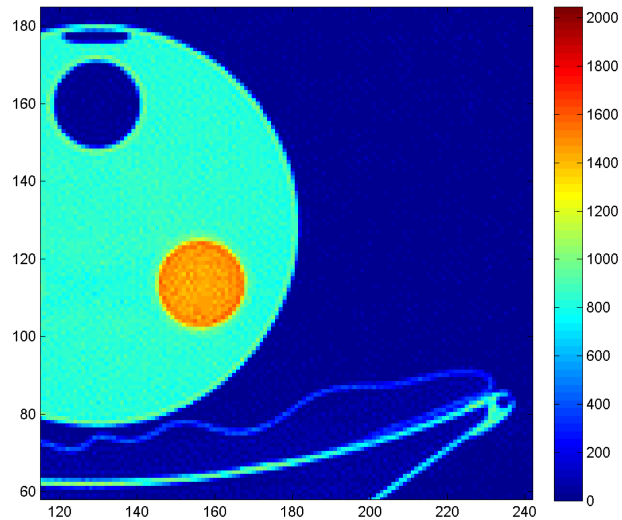

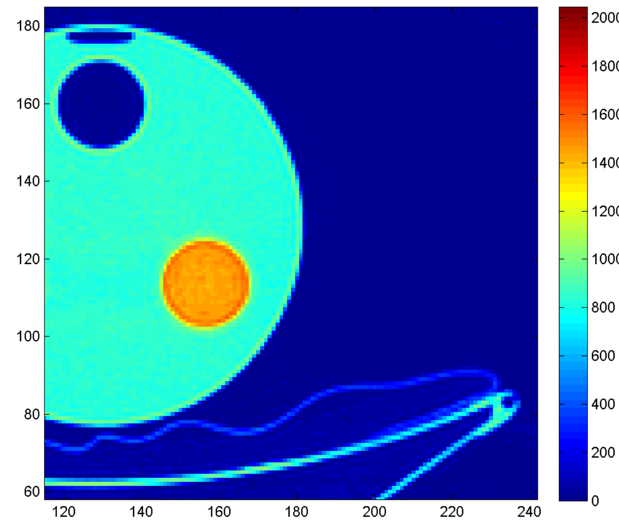

* POCS was stopped when computation time was approximately that of the deconvolution method and did not run to convergence.

Actual CT Noisy Reconstructed Images

- 385 slices; N=1536; M=512; P=1025; L=1690; $\lambda=1\times10^{-2}$; SNR=1.6dB *
- Filter over-determined by 1.5 **; Image over-determined by 2.9.
- Runtimes of FBP is 176s, POCS is 3.0s for 3 iterations, and Regularized Deconvolution is 2.3s.

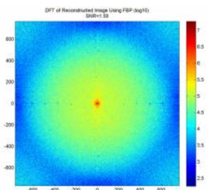

FBP DFT and Image

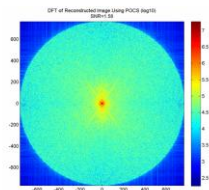

POCS DFT and Image

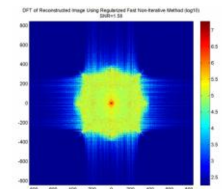

Reg. Deconv. DFT and Image

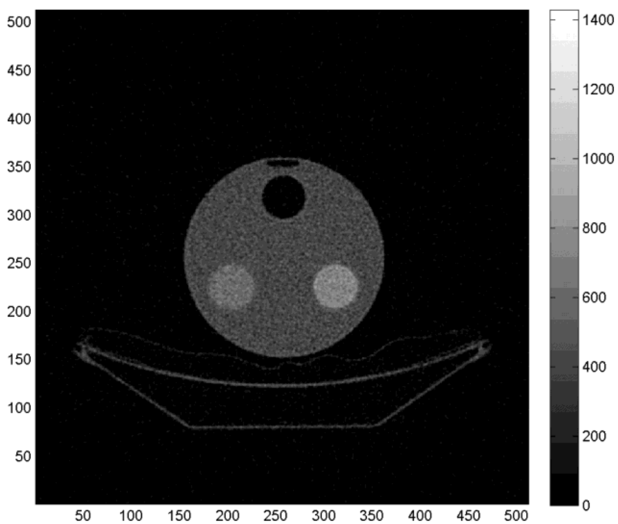

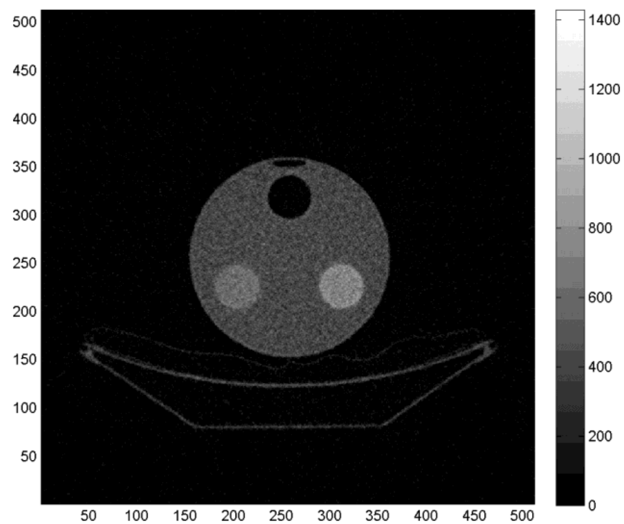

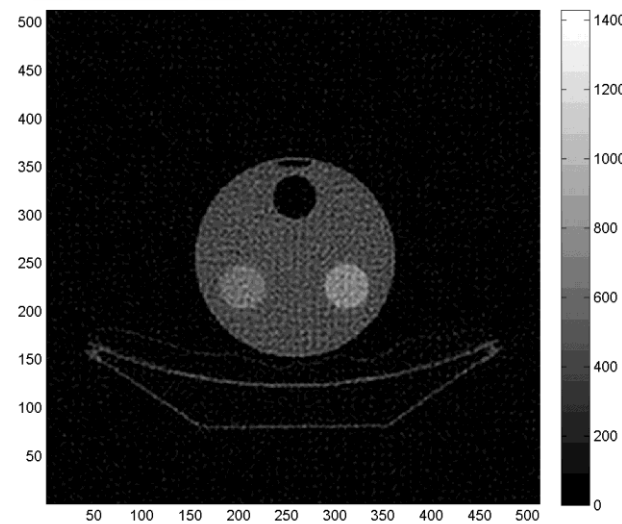

* Noise is zero-mean additive white Gaussian. ** Filter took 13 minutes to precompute offline.

Actual CT Large Reconstructed Images

- 667 slices; N=1332; M=888; P=445; L=1465; $\lambda=1\text{x}10^{-3}$; no noise.
- Filter over-determined by 3.7; Image over-determined by 1.3.
- Runtimes of FBP is 233s, POCS is 3.6s for 3 iterations, and Regularized Deconvolution is 4.7s.

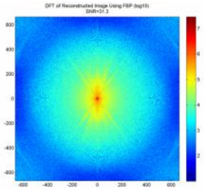

FBP DFT and Image

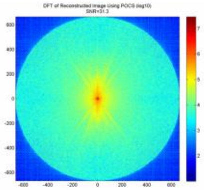

POCS DFT and Image

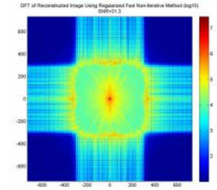

Reg. Deconv. DFT and Image

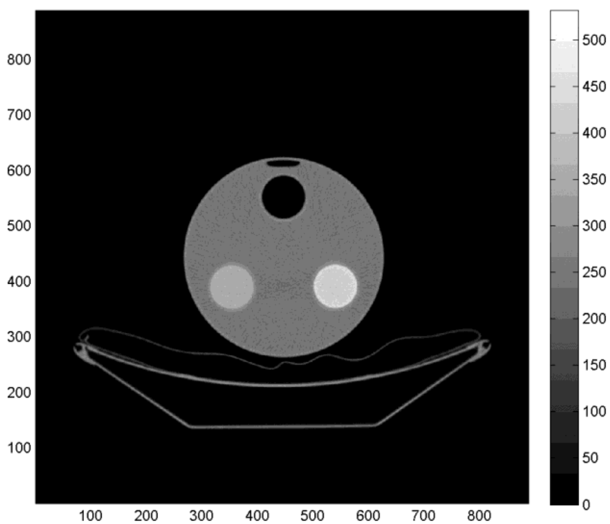

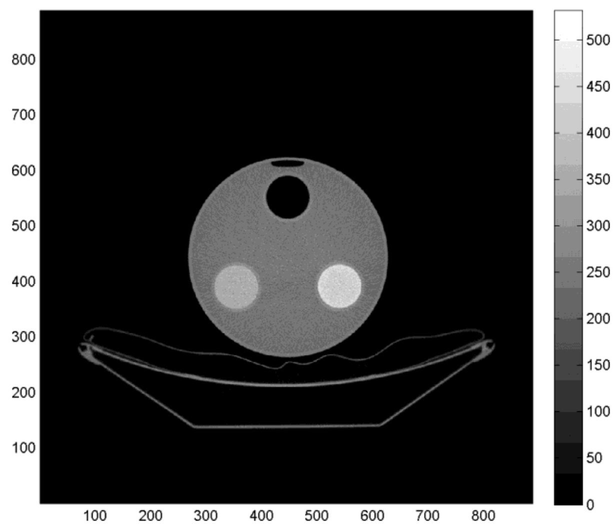

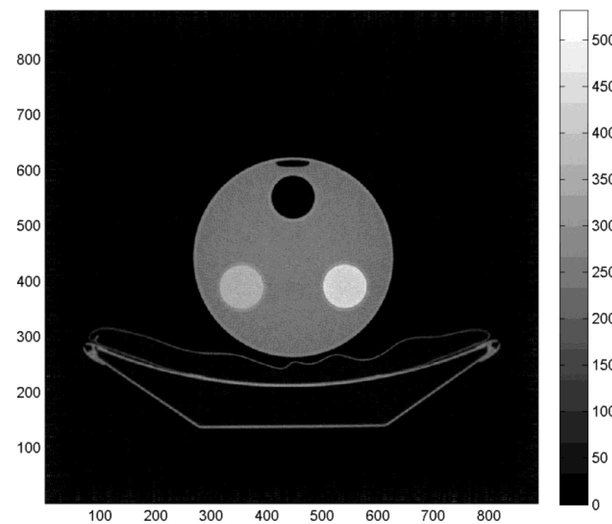

Overview

- Problem
- Conditioning Approach
- Non-Iterative Approach
- **Divide-and-Conquer Approach**
- Conclusion

Why Divide and Conquer?

- A large problem is replaced with similar smaller problems.
  - 1 image sized $N=256^2$ solved in $O(N^2)$ takes $1 \times 256^4=4.3\times10^9$ ops.
  - 64 subproblems each sized $N=32^2$ takes $64 \times 32^4=6.7\times10^7$ ops.
- Each subproblem can be regularized independently, depending on its conditioning.
  - Poorly conditioned or underdetermined subproblems (not enough frequency samples in that subband) can be discarded altogether, regularizing the overall problem.
- An unaliased low-resolution image can be reconstructed using the lowest-frequency subband.
  - This may be sufficient for recognition in some applications.
- Problem statement is same as earlier where the image is reconstructed from some values of its 2-D DTFT.

Divide Step: Gabor Logons

- Problem Formulation (Divide)
  1. Divide 2D frequency plane into $(2^K)^2$ subbands.
  2. Construct an over-complete set of modified 2D discrete-time Gabor logons truncated to ensure finite-support in time

$$\phi(i_1, i_2; k_1, k_2, \sigma) = \frac{1}{2\pi\sigma^2} e^{\frac{-(i_1^2+i_2^2)}{2\sigma^2}} e^{\frac{j2\pi(k_1 i_1 + k_2 i_2)}{2^K}}$$

$$k_1, k_2 = 0, \ldots, 2^K - 1, \quad \sigma = \frac{1}{\alpha_{overlap}} 2^K$$

  3. Project image onto modified Gabor logons
  4. Demodulate problem to baseband
  5. Downsample by k_1 and k_2 in each dimension.

2-D DTFT

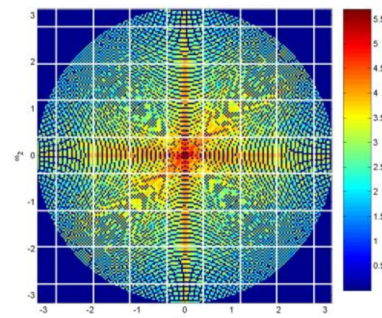

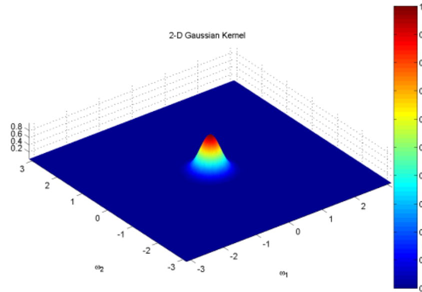

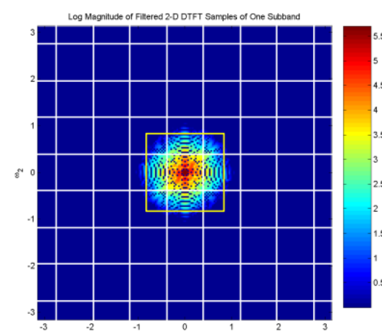

Conquer Step: Subband Subproblems

- Reconstruction (Conquer)
  6. Solve each self-contained subproblem separately and in parallel.

$$A_{k_1,k_2} \cdot y_{k_1,k_2}(i_1,i_2) = b_{k_1,k_2}$$

  7. Deconvolve each subsolution from downsampled Gabor logon

$$y_{k_1,k_2}(i_1,i_2) = x_{k_1,k_2}(i_1,i_2) ** \phi(i_1,i_2;k_1,k_2,\sigma)$$

  by point-wise division in the 2-D DFT domain.
  8. Combine all $(2^K)^2$ 2-D DFT subbands and inverse 2-D DFT to compute the original image.

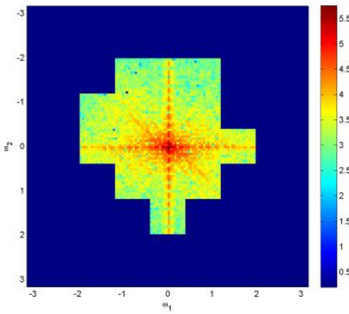

- Regularization
  - Uniform regularization may be applied.
  - Any badly conditioned subproblem can be regularized separately or even discarded if under-determined.

Simulation Data Uniform Regularization

- Simulation CT data with 128 slices each with 128 bins, divided in to $2^K x 2^K = 8x8$ (K=3) subbands, each of size 32x32 due to $\alpha_{overlap}=2$. M=128. SNR is 25.7 dB.
- Uniform regularization is $\lambda=1x10^1$.
- FBP RMSE=17.4 at 1.6s. D&C RMSE=2.92 at 1.6s / sub.

Original Image and DFT

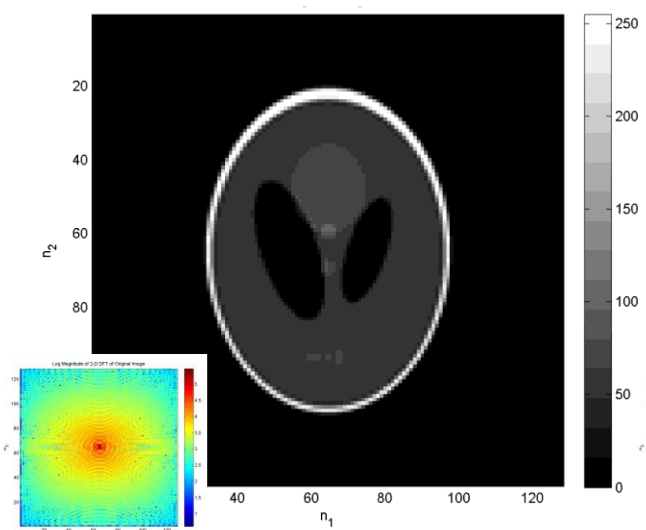

FBP Image and DFT

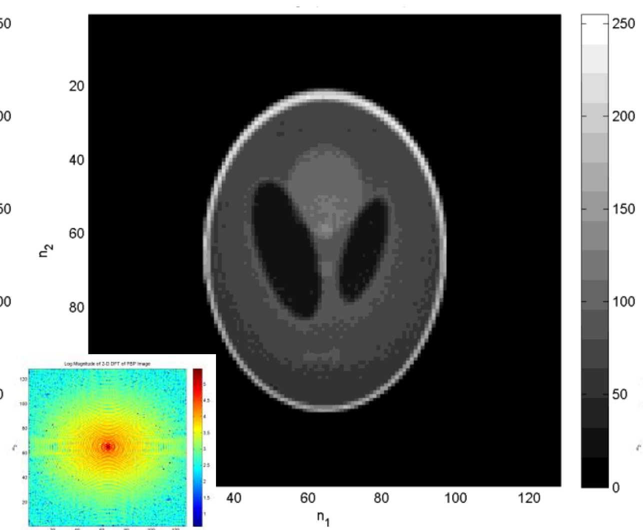

D&C Image and DFT

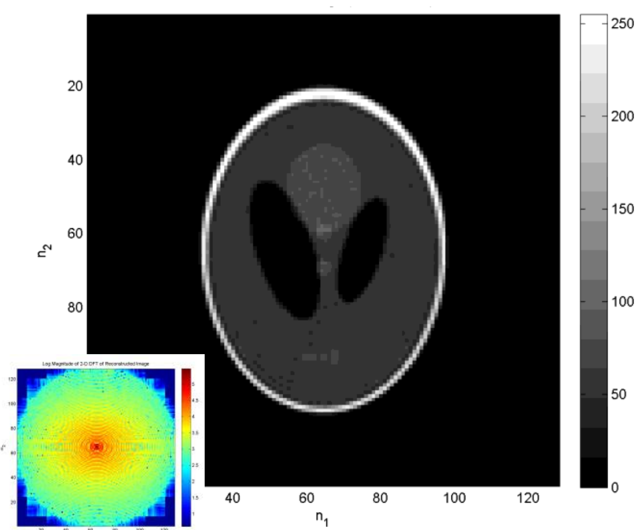

Simulation Data Variable Regularization

- Simulation CT data same as before. SNR is now 5.74 dB.
- Variable regularization from $\lambda = 1x10^{1}$ at lowest to $\lambda = 5x10^{1}$ at highest frequency subbands increasing log-linearly.
- FBP RMSE=22.3 at 1.8s. Var.D&C RMSE=13.1 at 1.5s/sub.
- D&C RMSE=13.5 ($\lambda = 1x10^{1}$). D&C RMSE=16.3 ($\lambda = 5x10^{1}$).

Original Image and DFT

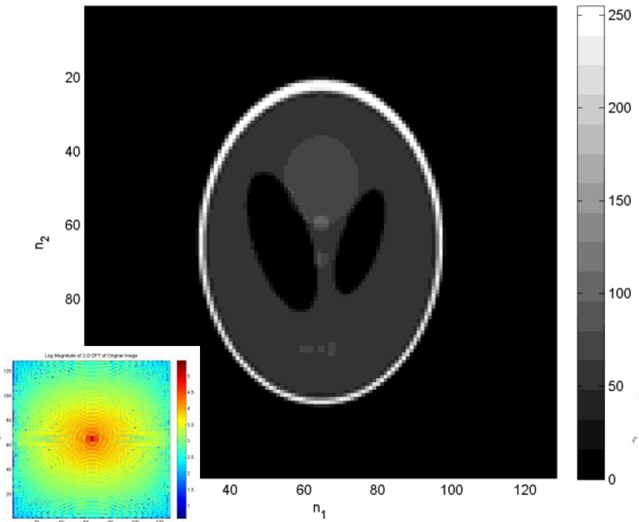

FBP Image and DFT

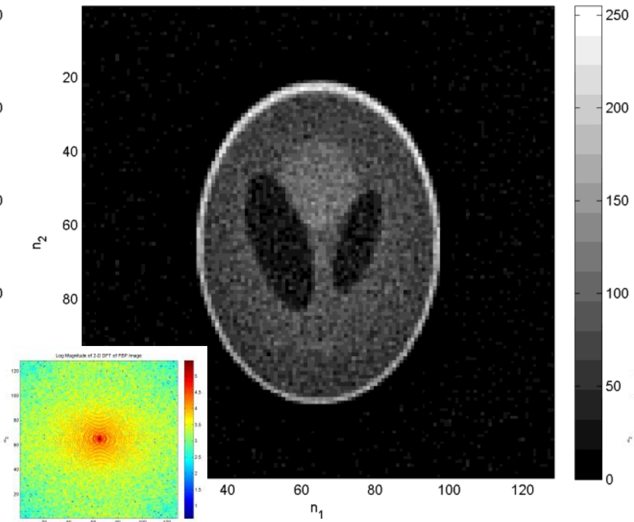

Var.D&C Image and DFT

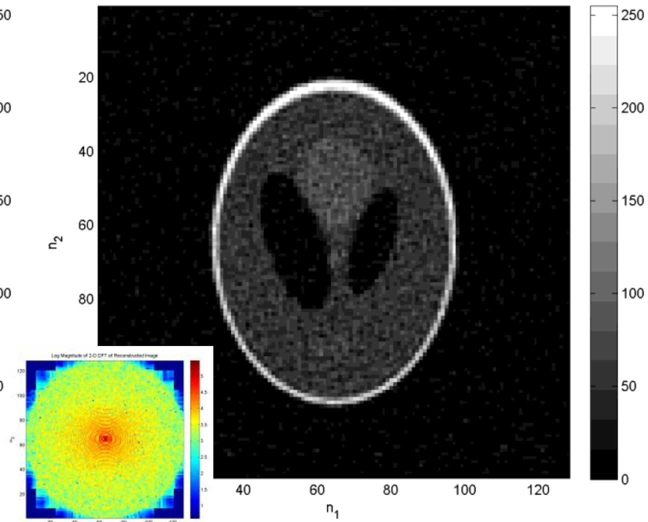

Actual CT Reconstructed Images

- Actual CT data with 205 slices each with 445 bins, divided in to $2^K x 2^K = 32x32$ (K=5) subbands, each size 32x32 with $\alpha_{overlap}=2$. M=512. SNR is 50.2 dB. Uniform $\lambda=1x10^0$.
- Runtimes of FBP is 10s, D&C is 0.7s / subproblem solved by PCG and 718s total.

FBP Image and DFT

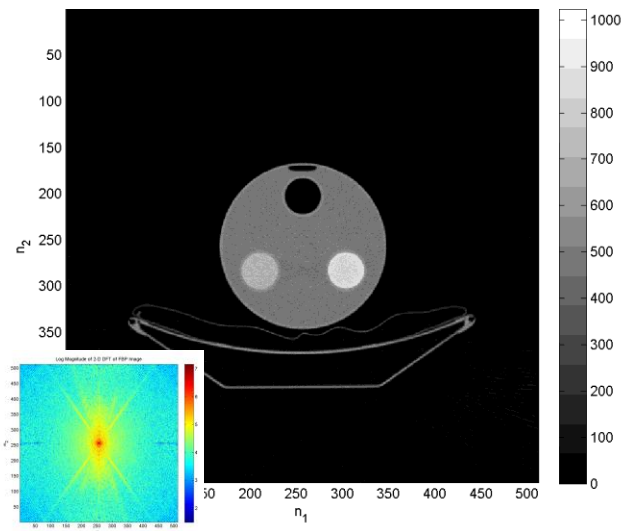

D&C Image and DFT

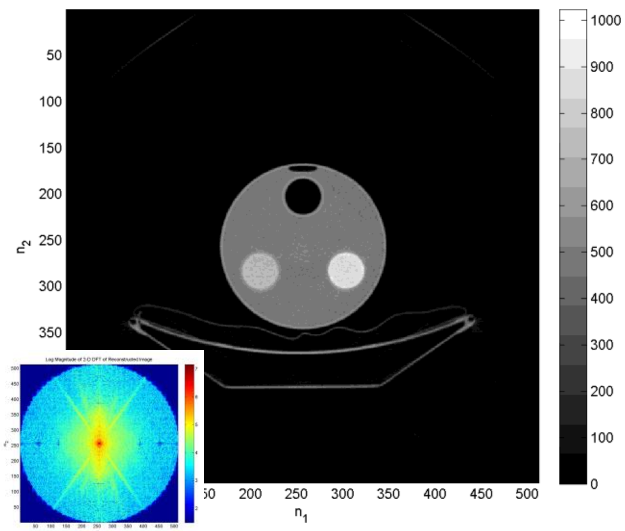

Lowest-Subband Image and DFT

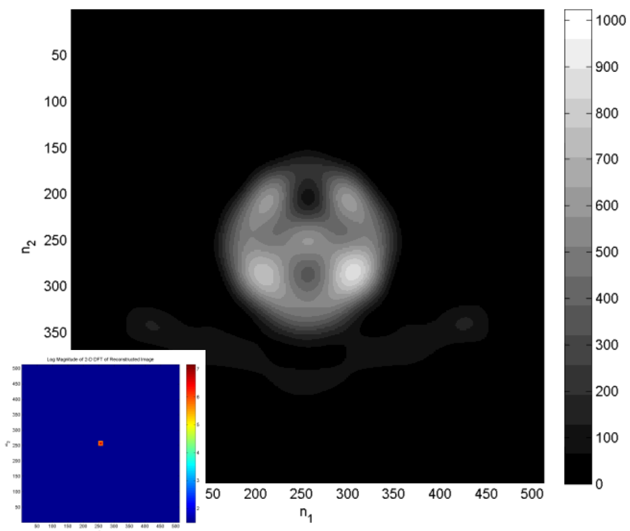

Overview

- Problem
- Conditioning Approach
- Non-Iterative Approach
- Divide-and-Conquer Approach
- **Conclusion**

Summary of Contributions

- Conditioning
  - Introduced a more efficient 45° rotated-support 2-D to 1-D unwrapping procedure which allows easier analysis of conditioning.
  - Developed a quick O(M) and accurate (r=0.80 with κ(A)) sensitivity measure of the variance of distances between 1-D DTFT locations, based on a closed-form formula for the upper-bound on the Frobenius condition number of a square Vandermonde matrix.

Summary of Contributions

- Algorithms
  - Developed a fast non-iterative algorithm that deconvolves a precomputed data masking filter from a filtered DFT of the data using just three 2-D DFTs.
  - Reinterpreted band-limited image interpolation as a finite-support regularization method for computing the data masking filter much faster than POCS.
  - Developed a procedure to sub-divide a reconstruction problem using Gabor logons and subband decomposition and applied varying regularization to each sub-problem.
- Numerical Results
  - Applied each of the conditioning, non-iterative, and divide-and-conquer methods to actual CT sinogram data with excellent reconstructions.

Evaluation of Results

- Conditioning
  - The variance measure is the only estimate of sensitivity reliable for the over-determined case and reduces the amount of regularization.
  - The Kronecker substitution based wrapping methods allow DTFT samples to be chosen more freely on parallel lines which was more restrictive in the Good-Thomas unwrapping. The helical scan FFT does not need a rotated support.
  - Frequency selection is achieved using simulated annealing with the variance measure when physical system geometry restrictions exist.
  - In applications like magnetic resonance spectroscopic imaging (MRSI) or 3-D MRI where data at each x-y sample is expensive, k-space trajectories maybe designed with a fixed number of samples with the best if not perfect conditioning without extra sampling.

Evaluation of Results

- Algorithms
  - The non-iterative approaches are recommended when frequency samples are already determined and fixed for multiple uses as we precompute the frequency mask filter once. The speed advantage comes from only requiring three 2-D FFTs.
  - The divide-and-conquer approach is also recommended for when sample locations are determined or when the image problem is large.
  - This subdivision allows customization of each subproblem in terms of regularization and the type of algorithm used to solve (closed-form, iteratively or non-iteratively) based on its conditioning.

Suggestions for Future Research

- The conditioning approaches may benefit from a stronger theoretical link between the fast sensitivity measures and the condition number which explain the strong empirical evidence relating the two quantities, especially in the overdetermined case.
- The non-iterative method computes a very quick solution, which in cases when resources are available, can be further refined with iterative methods.
- As for the advantage of the divide-and-conquer method, a non-aliased low-resolution image is quickly computed which can then be updated with higher resolution subbands.

Thank You!

Conditioning of and Algorithms for Image Reconstruction from Irregular Frequency Domain Samples

Benjamin C. Lee

Dissertation Oral Defense
May 10, 2010

University of Michigan
Electrical Engineering: Systems
Chair: Prof. Andrew Yagle